Structural investigation of ductile deformations across the Frontal Wedge south of Lake Vättern, southern Sweden

Ellinor Halvarsson

Dissertations in Geology at Lund University,
Master's thesis, no 644
(45 hp/ECTS credits)

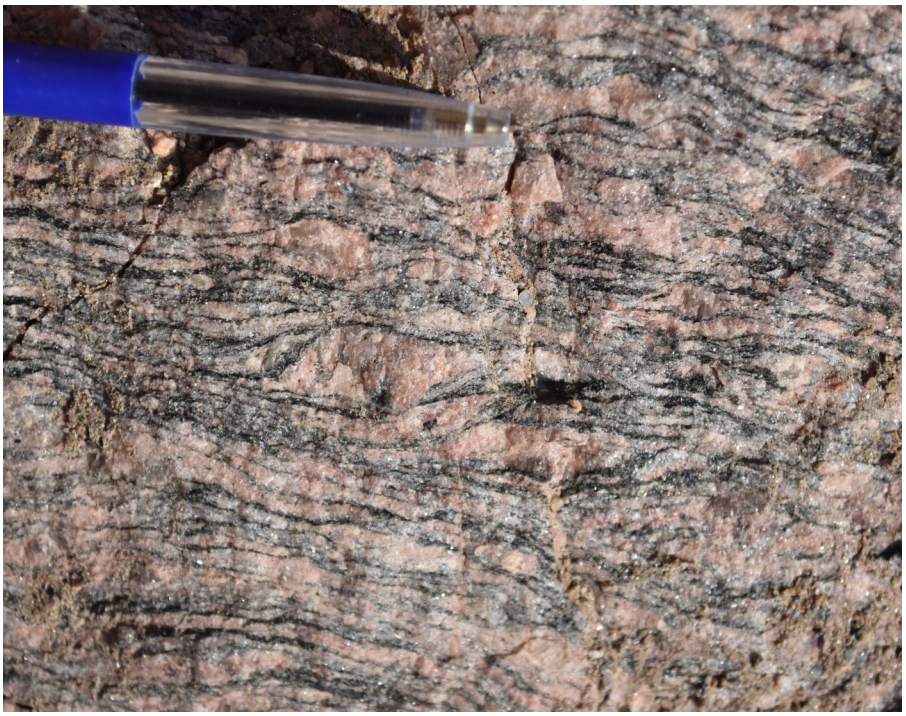

Department of Geology
Lund University
2022

Structural investigation of ductile deformations across the Frontal Wedge south of Lake Vättern, southern Sweden

Master's thesis

Ellinor Halvarsson

Department of Geology
Lund University
2022

Contents

1 Introduction **7**
2 Shear sense indicators **7**
2.1 Porphyroclast systems 7
2.2 Mineral fish and sigmoids 8
2.3 Shear bands and S-C fabric 8
3 Regional setting **8**
3.1 The Sveconorwegian Orogen 8
3.2 The Frontal Wedge 10
4 Method **11**
5 Results **11**
5.1 Field observations 15
5.1.1 The Eastern subarea 15
5.1.1.1 Ubbarp quarry 15
5.1.1.2 Hok 1 15
5.1.1.3 Hok Öst 15
5.1.1.4 Hok 2 15
5.1.1.5 Hok Väst 15
5.1.2 The Central subarea 15
5.1.2.1 Possarp 15
5.1.2.2 Målskog 15
5.1.2.3 Smörvik 15
5.1.2.4 Skjutebo 17
5.1.2.5 Boarp quarry 17
5.1.2.6 Tröjebo 17
5.1.2.7 Röshult 17
5.1.2.8 Flahult 17
5.1.3 The Western subarea 17
5.1.3.1 Munkabo 17
5.1.3.2 Arvidabo 17
5.1.3.3 Bottnaryd 20
5.2 Petrography 21
5.2.1 The Eastern subarea 21
5.2.2 The Central subarea 21
5.2.3 The Southern subarea 21
6 Interpretation and discussion **25**
7 Conclusions **27**
8 Acknowledgements **27**
9 References **27**

Cover Picture: Feldspar porphyroclast with asymmetric tails in gneissic rock. Photo: Ellinor Halvarsson.

Structural investigation of ductile deformations across the Frontal Wedge south of Lake Vättern, southern Sweden

ELLINOR HALVARSSON

Halvarsson, E., 2022: Structural investigation of ductile deformations across the Frontal Wedge south of Lake Vättern, southern Sweden. *Dissertations in Geology at Lund University*, No. 644, 29 pp. 45 hp (45 ECTS credits).

Abstract: The Frontal wedge is a system of N-S trending steep to vertical deformation zones at the border between the Sveconorwegian and Svecokarelian provinces in south-central Sweden. The origin of these structures is not fully understood and few investigations have been done on these deformation zones during the past decades. There are various interpretations of and models for the formation of the structures within the Frontal wedge. This study seeks to add field documentation from an area south of Lake Vättern with the aim to improve the understanding of the structure and its development. The field-based documentation includes structural measurements of the gneissic foliations, interpretation of shear-sense indicators, and petrographic documentation of the rocks across the Frontal wedge. This study also includes a comparison between the structure south of Lake Vättern with the structure north of lake Vättern described by Wahlgren et al. (1994). The results show that steep to vertical west-dipping deformation zones along an approximate E-W transect define a fan- or wedge-like structure with consistent western-block-up kinematics. Petrographic studies indicate that recrystallization of feldspar and penetrative deformation generally increases from east to west. The overall structural geometry in the studied area south of Lake Vättern resembles that described further north. The herein preferred model for the development of the Frontal wedge south of Vättern is that the structures originate from zones of weakness along intrusions formed before the Sveconorwegian orogeny. These zones were reactivated during the orogeny and the late-orogenic exhumation of the Eastern Segment and resulted in the formation of steep deformation zones with western-block-up kinematics. This model agrees with the observed structural geometry and especially the dominating vertical to near-vertical deformation zones. It is also in agreement with the kinematics derived from shear-sense indicators, and the gradational change in the character of the deformation of rocks from east to west in the study area south of lake Vättern.

Keywords: Frontal wedge, deformation zone, Sveconorwegian orogeny, shear-sense indicators, Protogine zone, structural geology

Supervisor(s): Charlotte Möller (LU) & Ulf Söderlund (LU)

Subject: Bedrock Geology

Ellinor Halvarsson, Department of Geology, Lund University, Sölvegatan 12, SE-223 62 Lund, Sweden. E-mail: el1602ha-s@student.lu.se / ellinor.halvarsson853@gmail.com

Strukturgeologiska undersökningar av duktila deformationer tvärs över ”Frontal Wedge” söder om Vättern, södra Sverige.

ELLINOR HALVARSSON

Halvarsson, E., 2022: Strukturgeologiska undersökningar av duktila deformationer tvärs över ”Frontal Wedge” söder om Vättern, södra Sverige. *Examensarbete i geologi vid Lund Universitet*, Nr. 644, 29 sid. 45 hp.

Sammanfattning: Deformationszonen kallad ”Frontal wedge” är ett system av N-S branta och vertikala deformationszoner i gränsen mellan Svekonorvegiska och Sekorareliska provincen, i södra Sverige. Ursprung av dessa strukturer är inte fullt förstått och under de senaste årtiondena har endast ett fåtal undersökningar gjorts på dessa deformationszoner. Det finns flera olika tolkningar och modeller för bildandet av strukturerna i ”Frontal wedge”. Denna studie syftar att bidra med fältdokumentation av ett område söder om Vättern för att förbättra förståelsen för strukturerna och deras uppkomst. Den fältbaserade dokumentationen inkluderar strukturgeologiska mätningar av foliationsplan, tolkning av kinematiska indikatorer och petrografiska studier på bergarter tvärs över ”Frontal wedge”. Denna studie inkluderar även en jämförelse mellan strukturerna som studerats söder om Vättern och de norr om Vättern beskrivna av Wahlgren et al (1994). Resultaten påvisar att branta till vertikala deformationszoner tvärs över strykningen definierar en ”solfjäder”- eller ”wedge”-struktur med konsekvent västra-blocket-upp kinematik. De petrografiska undersökningarna indikerar vidare att omkristallisation av fältspater och penetrativ deformation ökar från öst till väst i det studerade området. Den generella strukturen söder om Vättern liknar den som tidigare har beskrivits norrut. Den förespråkade modellen här, för utvecklingen av ”Frontal wedge” söder om Vättern, är att svaghetszoner bildade före Svekonorvegiska orogenesen är ursprunget för utvecklingen av ”Frontal wedge”. Dessa svaghetszoner reaktiverades under orogenesen och det påföljande upplyftandet av Östra Segmentet resulterade i bildandet av den branta deformationszonrema med västra-blocket-upp kinematik. Denna modell överensstämmer med den observerade strukturella geometrin, speciellt de dominerande branta till vertikala deformationsstrukturerna samt kinematiken härledd från kinematiska indikatorer och den gradvisa förändringen av deformationens karaktär i bergarterna från öst till väst i det studerade området.

Nyckelord: Frontal wedge, deformationszon, Svekonorvegiska orogenesen, kinematiska indikatorer, Protoginzonen, strukturgeologi

Handledare: Charlotte Möller (LU) & Ulf Söderlund (LU)

Ämnesinriktning: Berggrundsgeologi

Ellinor Halvarsson, Geologiska institutionen, Lunds Universitet, Sölvegatan 12, 223 62 Lund, Sverige. E-post: el1602ha-s@student.lu.se / ellinor.halvarsson853@gmail.com

1 Introduction

The easternmost part of the Sveconorwegian Province south of lake Vättern is characterized by a 20 – 30 km wide belt of approximate N-S trending anastomosing deformation zones (e.g., Wahlgren et al 1994; Möller et al 2015), traditionally referred to as the Protogine Zone (e.g. Andrésson & Rodhe 1990). A few studies have investigated these structures north (Wahlgren et al 1994) and south of lake Vättern (Andréasson & Rodhe 1990). N-S trending, steep to vertical faults, and narrow shear zones are described south of lake Vättern (Andréasson & Rodhe 1990) and deformation zones in a fan-shaped structure across the strike are described north of Lake Vättern (Wahlgren et al 1994). How these structures were formed is however yet to be resolved, but various models of the development have been proposed, including extensional (Andréasson & Rodhe 1990) and collisional settings (e.g., Burke et al 1977; Falkum & Petersen 1980). One model suggests that a younger set of deformation led to the rotation of older deformation zones in a compressional regime and caused the development of a fan-shaped structure (Wahlgren et al 1994; Stephen et al 1996; Juhlin et al 2000). Other studies argue that the deformation zones originates from structures older than the Sveconorwegian orogen and that movements along these structures during the uplift of the Eastern Segment formed the belt of deformation zones, i.e., the Frontal wedge, in an extensional regime (Andreasson & Rodhe 1990; Gorbatschev & Bogdanova 2000; Söderlund et al 2005).

Andréasson & Rodhe (1990) uses the traditional term 'Protogine Zone' south of lake Vättern, whereas Wahlgren et al (1994) suggested that this term should be avoided. Wahlgren et al (1994) introduced the term Sveconorwegian frontal deformation zone (SFDZ) comprising younger, discrete, and west-dipping deformation zones north of lake Vättern, with a reversed and right-lateral horizontal component of movements. They suggest that the SFDZ should be used also south of lake Vättern for similar structures. However, more recent studies have applied the term "Frontal wedge" (Möller et al 2015; Möller & Andersson 2018; Weller et al 2021) or, loosely, "boundary zone" (Ulmius et al 2018). These terms refer to the vertical to steeply west-dipping deformation zones with west-side-up kinematics that collectively form a sub-vertical wedge or fan structure (Möller et al 2015; Möller & Andersson 2018; Ulmius et al 2018).

In this study, I use the term "Frontal wedge" as defined by Möller et al (2015). I have chosen to use the term "Frontal wedge" since it refers to the position of the steep to vertical west-dipping deformation zones within the Eastern Segment, both north and south of Lake Vättern. By studying the deformation structures along an approximate E-W transect across the Frontal wedge south of lake Vättern, this project aims to add new data and field documentation on the Frontal wedge, and thereby contribute to further understanding of the tectonic evolution and origin of the Frontal wedge. The results are also compared to the structures north of lake Vättern (e.g. Wahlgren et al 1994), to investigate if these northern structures continue further south.

2 Shear sense indicators

Shear sense indicators, also known as kinematic indicators, are asymmetric small-scale structures that record relative movements in deformation zones. These structures develop during progressive deformation and have geometries that ideally reveal the sense of movement during deformation (Fig 1). There are multiple types of shear-sense indicators, depending on rock types, strain intensity, and metamorphic conditions. Shear-sense indicators develop on different scales: in outcrop, hand specimen, and at a microscopic level (Hanmer & Passchier 1991; Passchier & Trouw 2005). Below is a short review of selected shear-sense indicators which are relevant to this study.

2.1 Porphyroclast systems

Porphyroclasts are single larger clasts in a relatively fine-grained matrix. Commonly, porphyroclasts have polycrystalline rims or mantles of different compositions than the matrix. These mantled porphyroclasts are referred to as porphyroclast systems. The formation of porphyroclast systems starts with the development of a core-and-mantle structure. This process is caused by high differential stresses in the rim of the porphyroclast, resulting in local crystal-plastic deformation which further results in dynamic recrystallization of the rim, forming a mantle around the remaining poprhyroclast (Passchier & Simpson 1986; Passchier & Trouw 2005). With increased shear strain, the mantle will deform into tails on each side of the poprhyroclast (Fig 1a-b). Depending on the geometry of the developed tails, will it either form a σ-type, ϕ- type, δ-type, or a complex mantled type (with multiple tails) system (Passchier & Trouw 2005). The relevant systems for this study are the σ- and δ-types, since these are the ones found in the studied rocks (Fig 1a-b). The recrystallization rate versus the shear strain rate determines which one of the σ- and δ-type will form. If the recrystallization rate is high, σ-type systems are more likely to form, and, if low, δ-type systems will develop. Generally, δ-type systems will form at high shear strain and σ-type systems at lower shear strain (Passchier & Simpson 1986; Hanmer & Passchier 1991). The shape of the central core, i.e., the remaining porphyroclast, also influences which system will develop. δ-type systems commonly form when the clast is round or weakly elliptical whereas σ-type systems are more likely where the porphyroclast is elongated (Passchier & Simpson 1986).

Both σ-type and δ-type systems can be used as shear sense indicators due to the asymmetry of the tails. However, confusion between the two will result in erroneous inference of the opposite movement. The most characteristic feature of the δ-type is a bend of the tails at the contact of the porphyroclasts, creating a cusp of the matrix material. Furthermore, the tails of the σ-type always have stair-stepping geometry whereas the δ-type can occur without. The thickness of the tails is also different between the two types. The tails of the σ-type are wide nearest the porphyroclast and become thinner further away from each side of the porphyroclast whereas the tails of the δ-type are evenly thin (Passchier & Trouw 2005). When the type of the porphyroclast system is identified the "stair-

stepping" of the tail can be used to derive the shear sense. In a σ-type system, the upper tail will "step-up" in the direction of the movement of the upper block. In a δ-type system, the lower tail will "step up" to indicate the sense of displacement of the upper block (Passchier & Trouw 2005).

2.2 Mineral fish and sigmoids

Mineral fish are elongated or lens-shaped single crystals with the longest dimension at a small angle to the foliation (Fig 1c). These are commonly developed by white mica in mylonites, called mica fish. Other minerals, such as plagioclase, K-feldspar, biotite, and kyanite, can also form mineral fish structures. It is not fully understood how these structures develop (Hanmer & Passchier 1991). They may evolve through different processes such as internal deformation, resorption by recrystallization or pressure solution, or lateral growth by precipitation of dissolved material (Passchier & Trouw 2005).

Sigmoids, on the other hand, are elongated aggregates of minerals, without any porphyroclast core, in a matrix of other minerals (Fig 1d). Typically, the shape of sigmoids resembles the shape of mineral fish or σ-type poprhyroclasts. The development of sigmoids is not fully clear either. The structure may develop when σ-type boudins are separated from veins or form when σ-type poprhyroclast systems are fully recrystallized. Regardless of the formation of mineral fish structures and sigmoids, their stair-stepping shape can be used to determine the shear sense. The orientation of the elongation indicates the sense of displacement, meaning that the inclination of the top plane is indicative of the movement of the upper block (Fig 1c-d; Passchier & Trouw 2005).

2.3 Shear bands and S-C fabric

A composite fabric called S-C fabric, commonly formed in mylonitic rocks, can also be used to determine the shear sense. S-C fabric comprises two types of planes that develop simultaneously: a non-penetrative shear bands (C) and a penetrative foliation (S) (Fig 1e-f; Hanmer & Passchier 1991; Passchier & Trow 2005). The C-planes are narrow shear zones and develop when strain is heterogeneous in e.g., granitic rocks deformed at temperatures lower than the crystal-plastic limit of feldspars (Hanmer & Passchier 1991). The C-planes are connected with sigmoidal S-planes which will rotate towards the C-planes with increased strain (Hanmer & Passchier 1991). The C- and S-planes develop simultaneously, and the C-plane lies parallel to the shear zone boundary (Passchier & Trouw 2005) and the flow plane of the deformation (Hanmer & Passchier 1991). In some cases, a C'-type shear band will develop and overprint the S-C fabric, commonly in very foliated mylonites and mylonitic mica schists (Passchier & Trouw 2005). These shear bands are oriented about 12-25 degrees to the shear zone boundaries and the S-plane, i.e. the main foliation (Hanmer & Passchier 1991; Passchier & Trouw 2005). The development is only partly understood but C'-planes form when a strong mineral preferred orientation is already developed and when noncoaxial flow act along the plane of anisotropy (Passchier & Trouw 2005). The geometry of the C'-type shear bands can vary, but they are commonly shorter, wavier, and less continuous than C-type shear bands (Hanmer & Passchier 1991; Passchier & Trouw 2005). There are a few ways in which the shear sense can be indicated from shear bands and S-C fabrics. It can be derived from the angle between the shear bands and the S-plane (Passchier & Trouw 2005; Winter 2014), from the sigmoidal shape of the S-plane, and the angle between the C'-type shear bands and the shear zone boundary (Passchier & Trouw 2005).

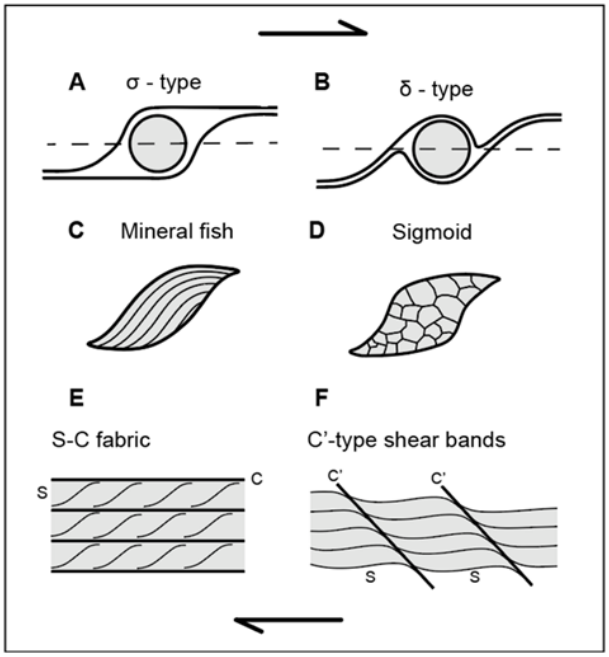

Fig. 1. Schematic illustration of the types of shear sense indicators used in this study, shown at a top-to-the-right movement on a horizontal shear plane (modified from Passchier & Trouw 2005). A) and B) Winged porphyroclasts C) and D) Sigmoidal minerals and mineral aggregates. E) and F) S-C type fabrics.

3 Regional settings

3.1 The Sveconorwegian Orogen

The Sveconorwegian Province is a 500 km wide orogenic belt in the Baltic Shield in southern Scandinavia (Fig 2; Möller & Andersson 2018; Bingen et al 2021). Accretionary (Coint et al 2015) and collisional events have been suggested for the formation of the Sveconorwegian Orogen (SNO; Möller & Andersson 2018; Bingen et al 2021; Weller et al 2021). The orogeny was part of the assembly of the supercontinent Rodinia at about 1.3- 0.9 Ga (Li et al 2008; Möller et al 2015; Möller & Andersson 2018) and the Sveconorwegian Orogen is suggested to be the tectonic counterpart of the Grenville Orogen in Laurentia (Möller et al 2015; Möller & Andersson 2018). The collisional model suggested for the orogeny, describe westward underthrusting of the Eastern Segment below the eastward advancing western Sveconorwegian domain (referred to as "Sveconorwegia" by Brueckner 2009; Möller & Andersson 2018). Extension and associated orogenic collapse began after 0.97 Ga, which also resulted in movements along major deformation zones in the SNO (Möller et al., 2015; Ulmius et al., 2018).

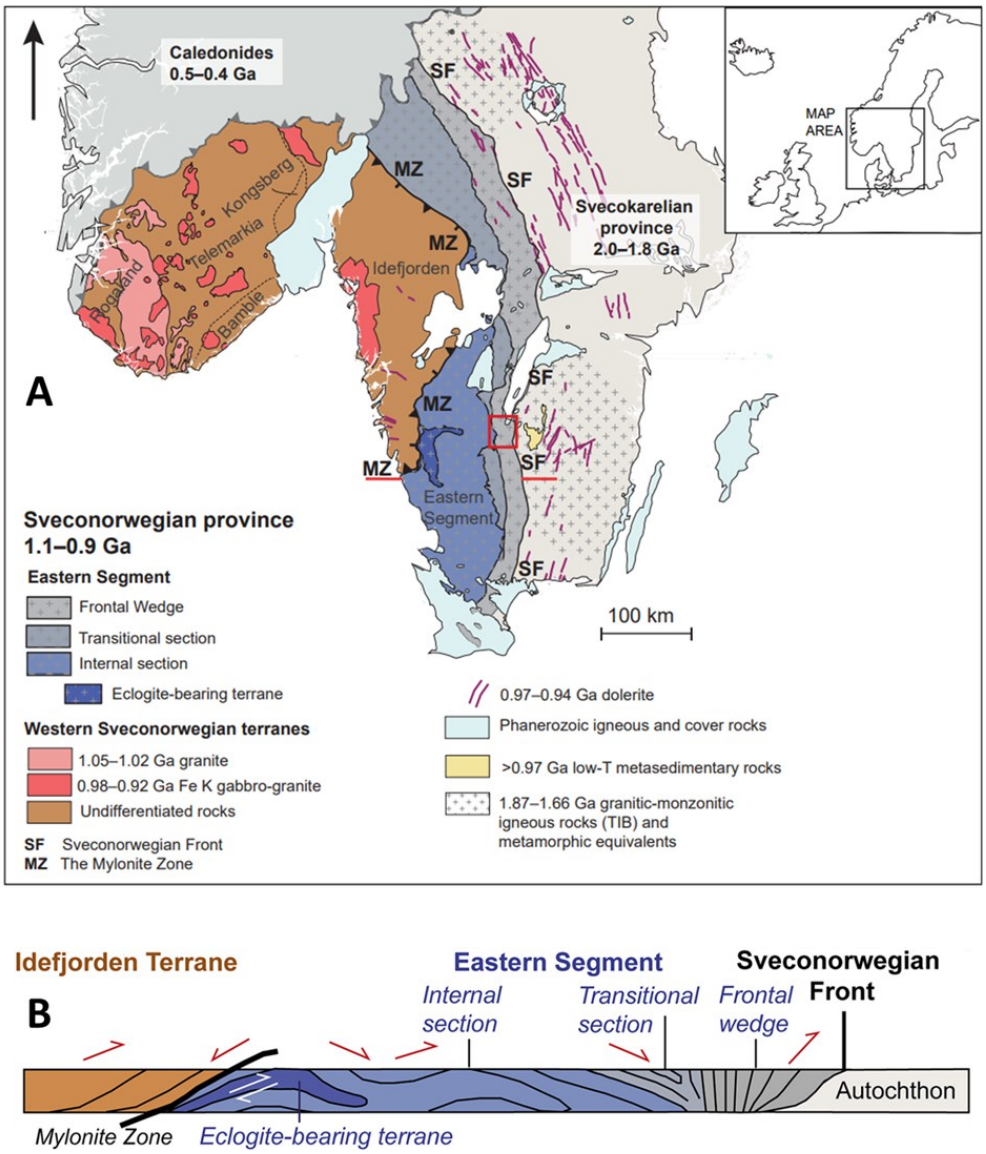

Fig. 2. A) Regional sketch map of the Sveconorvegian orogen (SNO). The Eastern Segment is in violet to dark medium grey shades. The Frontal Wedge is the grey zone immediately west of the Sveconorwegian Front (SF). The internal subdivision of the Eastern Segment is after Möller et al (2015). The red bars mark the location of the schematic cross-section (B). B) Schematic W -E cross-section of the SNO. Figures from Möller & Andersson (2018). The red box in (A) indicate the study area.

Today, only mid-to-upper crustal levels are exposed of the former 70-80 km thick (Möller & Andersson 2018; Weller et al 2021) and extensive mountain belt.

Two main stages of metamorphism are recorded in the bedrock of the Sveconorwegian Province (Möller et al 2015; Möller & Andersson 2018; Bingen et al 2021). The first stage is found in the western Sveconorwegian domain and is dated at 1.05 – 1.0 Ga (Bingen et al 2008a, 2021). The western Sveconorwegian domain comprises five terranes including the Idefjorden terrane, Bamble terrane, Kongsberg terrane, Telemarkia terrane, and Rogaland terrane, which are separated by ductile shear zones. Mid-crustal metamorphism is recorded dominantly in the western Sveconorwegian terranes. Bamble, Kongsberg, and parts of the Telemarkia terrane were parts of the upper crust during this event, and later downthrusted to their current position. Intrusion of high-K calc-alkaline granite magmas at about 1.07-1.02 Ga took place in Telemarkia. Metamorphism involved upper amphibolite metamorphism and migmatization at 1.04-1.00 Ga (Bingen et al 2021; and references therein), ultra-high metamorphism in Rogaland at 1.03-1.00 Ga (Laurent et al 2018), and high-pressure granulite-facies metamorphism in Idefjorden at about 1.05-1.02 Ga (Söderlund et al 2008; Bingen et al 2008b, 2021). This first stage of metamorphism has been proposed to be associated with pre- to syn-collisional settings due to the occurrence of calc-alkaline magmatism in the domain. (Weller et al. 2021, and references therein).

The second stage of metamorphism, at 0.99–0.97 Ga, is recorded in the Eastern Segment and is related to protracted collision during the underthrusting of the Eastern Segment beneath the western Sveconorwegian domain (Möller et al 2015, Möller & Andersson 2018). The Eastern Segment and western Sveconorwegian domain are separated by a wide ductile shear zone called the Mylonite Zone (MZ). This

shear zone is over 10 km wide, about 450 km long, and has a general gentle westward dip (Viola et al 2011; Möller et al 2015). The bedrock of the Eastern Segment was originally part of the Transscandinavian Igneous Belt (TIB), dated at 1.85-1.66 Ga (Högdahl et al 2004; and references therein). The Eastern Segment consists of granitic rocks grading into granodiorite, quartz-monzonite, and quartz-monzodiorite, but gabbroic rocks occur as well (Möller et al 2015; Möller & Andersson 2018). There is a progressive transition from greenschist- and epidote amphibolite-facies in the east to high-pressure granulite-facies in the west (Möller & Andersson 2018; Urueña et al 2021). An eclogite-bearing nappe is exposed immediately beneath the Mylonite Zone (Möller et al 2015). The eclogite- and high-pressure granulite- to amphibolite-facies metamorphic events are dated at 0.99 and 0.98–0.97 Ga, respectively (Möller et al 2015; Beckman et al 2017). The Eastern Segment has been divided into three sections based on the transition in metamorphic grade and the style of deformation: the Frontal wedge in the east, the Transitional section west thereof, and the Internal section in the west (Möller et al 2015). The easternmost part of the orogen (the Frontal wedge) is a steep wedge-like structure characterized by non-penetrative deformation along dominantly vertical deformation zones (Andréasson & Rodhe 1990; Möller & Anderssson 2018). The metamorphic grade in the transitional section is amphibolite-facies and the rocks are penetratively deformed and gneissose. Amphibolite-facies felsic gneisses hosting garnet amphibolite and metagabbro, km-scale folding of the bedrock, and remnants of relict igneous textures are other characteristics of the transitional section. The internal section is characterized by high metamorphic grade and abundance of migmatitic meta-granitic and -gabbroic rocks. The metamorphic grade reaches up to high-pressure granulite- and upper amphibolite-facies and the deformation is near-penetrative. Lenses and layers of garnet amphibolite, high-pressure mafic granulite, and folding of the high-grade gneissic layers are also present in the internal section. The eclogite-bearing nappe at the contact between the Eastern Segment and western Sweconorwegian domain forms a recumbent fold that carries eclogite and retrogressed eclogite. The nappe underwent tectonic burial during underthrusting below the western Sveconorwegian domain and later exhumation with retrogression (Möller et al 2015).

3.2 The Frontal Wedge

The Frontal wedge is an approximate 20-30 km wide belt of discrete deformation zones that extends from Scania to central Sweden, where it disappears below the Scandinavian Caledonides (Fig 2a). South of Lake Vättern, the Frontal wedge is characterized by steep to vertical deformation zones and rocks with non-penetrative deformation (Andréasson & Rodhe 1990; Möller & Andersson 2018). The dip direction changes from west in the eastern part of the Frontal wedge, over vertical, to east in the transitional section (Fig 2b; Andréasson & Rodhe 1990; Wahlgren et al 1994; Möller et al 2015). Normal movement of the western deformation zones and reversed movement of the eastern deformation zones, can be linked to the uplift of the western high-grade parts of the Eastern Segment (Andréasson & Rodhe 1990; Wahlgren et al 1994). The metamorphic grade changes from unmetamorphosed or greenschist-facies in the east to amphibolite-facies in the west (e.g., Johansson & Johansson 1990; Andréasson & Rodhe 1990: Wahlgren et al 1994; Möller & Andersson, 2018). The increase in metamorphic temperature is in agreement with recrystallization of feldspar in the western areas in contrast to eastern locations (e.g., Urueña et al 2021). Other features documented in association with the Frontal wedge are a regional gravity low trending from the northern Scania, to and beyond the Caledonian front (Johansson 1990; Henkel 1992) and a N-S trending banded pattern of magnetic anomalies (Fig 3; Wikman 2000; Wik et al 2006).

The bedrock within the Frontal wedge south of Vättern comprises a variety of rock types which are mainly reworked varieties of the Transcandinavian Igneous Belt (TIB) rocks (Wik et al 2006). Granitic rocks, such as quartzmonzonite, quartzmonzodiorites, granodiorites, and tonalites, are the dominating intrusive rocks (Wikman 2000; Wik et al 2006), dated at 1.85 Ga to 1.66 Ga (Högdahl et al 2004; and references therein); volcanic rocks are present but in lesser amount (Wikman 2000). In highly deformed areas, the granitic rocks are fine-grained with partly to fully recrystallized feldspar augen. S-C fabric and winged K-feldspar porphyroclasts are common in the deformed granitic rocks (Andréasson & Rodhe 1990; Wahlgren et al 1994; Wik et al 2006).

Metagabbro and amphibolites are present in the Frontal wedge. Where strongly deformed, mafic rocks are transformed into biotite- and chlorite-rich schists (Wik et al 2006). Multiple generations of metagabbro and metadolerite occur within the Frontal wedge (Söderlund & Ask 2006; Wik et al 2006). The oldest generation is dated at about 1.57-1.56 Ga and form irregularly shaped bodies both north (Wahlgren et al 1996; Söderlund et al 2005) and south of Lake Vättern (Ask 1996; Söderlund et al 2005). The same generation of metagabbro is present in the Transitional section (Beckman et al., 2017). Other generations of variably metamorphosed basic magmatic rocks include dolerite, gabbro and anorthosite which are 1224–1215 Ma old (Berglund et al 1997; Jarl 2002; Söderlund et al 2005; Söderlund & Ask 2006), and 1204 Ma old (Johansson 1990; Hansen & Lindh 1991; Söderlund & Ask 2006). The largest intrusion related to the ca. 1.2 Ga magmatism is the elongate Vaggeryd syenite, located in the central Frontal wedge south of Vättern. It trends N-S and comprises mainly of quartz syenite and syenite and is affected by N-S trending deformation zones, especially along its margins to the TIB gneisses (Söderlund & Ask 2006; Wik et al 2006). The youngest generation of mafic intrusions belongs to the Blekinge-Dalarna dolorites (BDD), which intruded at 0.98-0.95 Ga (Söderlund et al 2004; Söderlund et al 2005).

Various tectonic models have been proposed for the deformation structures along the Frontal wedge. In early studies, the structures were suggested to represent a collisional suture zone (e.g., Burke et al 1977; Falkum & Petersen 1980). Wahlgren et al (1994) also argues for an origin related to a compres-

sive event but suggest that two superposed events have caused the fan-like structure. They suggest that a Sveconorwegian or older imbricate thrust stack with easterly dip, was cross-cut by a younger west-dipping deformation zone with reversed and right-lateral horizontal component of movement (SFDZ). This led to rotation of the older thrust stack into the westward dipping SFDZ (Wahlgren et al 1994; Juhlin et al 2000). Stephens et al (1996) suggests that this late deformation (SFDZ) with a right-lateral horizontal shear component marked the decline of the crustal shortening during the Sveconorwegian orogeny.

Andréasson & Rodhe (1990) suggest, however, an extensional origin involving incipient rifting of thinned crust along Sveconorwegian or older structures, which resulted in the development of a half-graben complex. Continued extension is proposed to have been followed by unroofing and isostatic rebound of the high-grade metamorphosed crust in the west (Andréasson & Rodhe 1990). Other studies argue that the Frontal wedge originates from structures relating to the 1.57 and 1.2 Ga intrusive rocks, i.e., structures older than the SNO (e.g., Johansson & Johansson 1990; Johansson 1990; Söderlund et al 2005; Söderlund & Ask 2006). It is proposed that zones of crustal weakness formed in relation to these pre-Sveconorwegian intrusive events and that these zones were reactivated during the Sveconorwegian orogeny (Gorbatschev & Bogdanov 2000; Söderlund et al 2005; Söderlund & Ask 2006). Furthermore, Söderlund et al (2005) suggest that the later decline of the orogenic activity was followed by isostatic rebound and exhumation of the western Eastern Segment. This led to extensional movements along the Frontal wedge and the formation of the characteristic deformation structures (Söderlund et al 2005).

4 Methods

Fieldwork was done for 2 weeks in July 2021 in central Småland, south of lake Vättern (Fig 4). The main objective was to document and measure structures across the Frontal wedge. In total, 16 localities were visited (Fig 4). These localities were selected because, firstly, they approximately cover the central Frontal wedge and, secondly, because the bedrock is relatively well exposed in these areas. The coarse-grained Barnarp gneiss is the dominating lithology south of lake Vättern and is suitable for structural analysis. In the westernmost part (locality Bottnaryd) of the study, area measurements were made on a mafic rock since no felsic gneiss was found. The amount of exposed bedrock and the possibility to make measurements varied significantly between outcrops and therefore the number of structural measurements vary between localities.

At all localities, the strike, dip, and dip direction of the foliation were measured using a Silva compass. Field observations and structural features were recorded with a focus on potential kinematic indicators, such as K-feldspar porphyroclasts with asymmetric tails and S-C fabric.

The structural data were then plotted as poles to the planes, in stereograms using the program Stereonet.

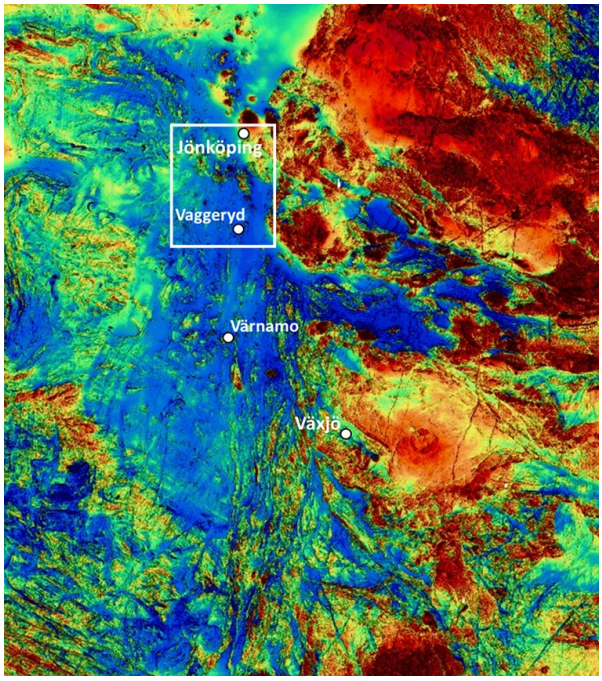

Fig. 3. Airborne magnetic anomaly map of a part of southern Sweden including the Frontal wedge south of Lake Vättern.The red and blue colors reflect high and low values of the total magnetic field, respectively (data source: Geological Survey of Sweden). N-S trending banded patterns of magnetic anomalies are typical for the Frontal wedge (Wik et al 2006). The white box defines the study area.

Sampling of the studied rock was successful at 4 localities including Hok 2, Hok Väst, Målskog, and Boarp (Table 1). The samples were aimed for thin section preparation and further study of shear sense indicators. All samples were sawed perpendicular to the foliation and parallel with the linear fabric and orientation marks were transferred to the rock chips. Additionally, thin sections from Urueña et al (2021) and thin sections from Perälä (2018) were studied (Table 1). The samples from Urena et al (2021) were gathered within the study area of this work. The samples from Perälä (2018) were also gathered within the boundaries of the Frontal wedge south of lake Vättern, however about 44 km south of the present study area (Fig 4). A Nikon Eclipse E400 polarizing microscope was used for the petrographic investigation of the thin sections. For the oriented thin sections, kinematic indicators were used for determining the shear sense direction (Table 1).

5 Results

The investigated localities are marked in Figure 4, together with structural data. Figure 5 shows a schematic profile of the measured dip direction and Figure 6 the structural data for each locality in stereograms. Table 1 lists coordinates, the thin sections studied, structural data, and the shear sense direction. The localities related to this study, including those of Urueña et al (2021) and Perälä (2018), are divided into subareas based on their geographical location; the eastern subarea (blue), the central subarea (red), the western subarea (green) and the southern subarea (grey) for the samples from Perälä (2018) (Fig 4).

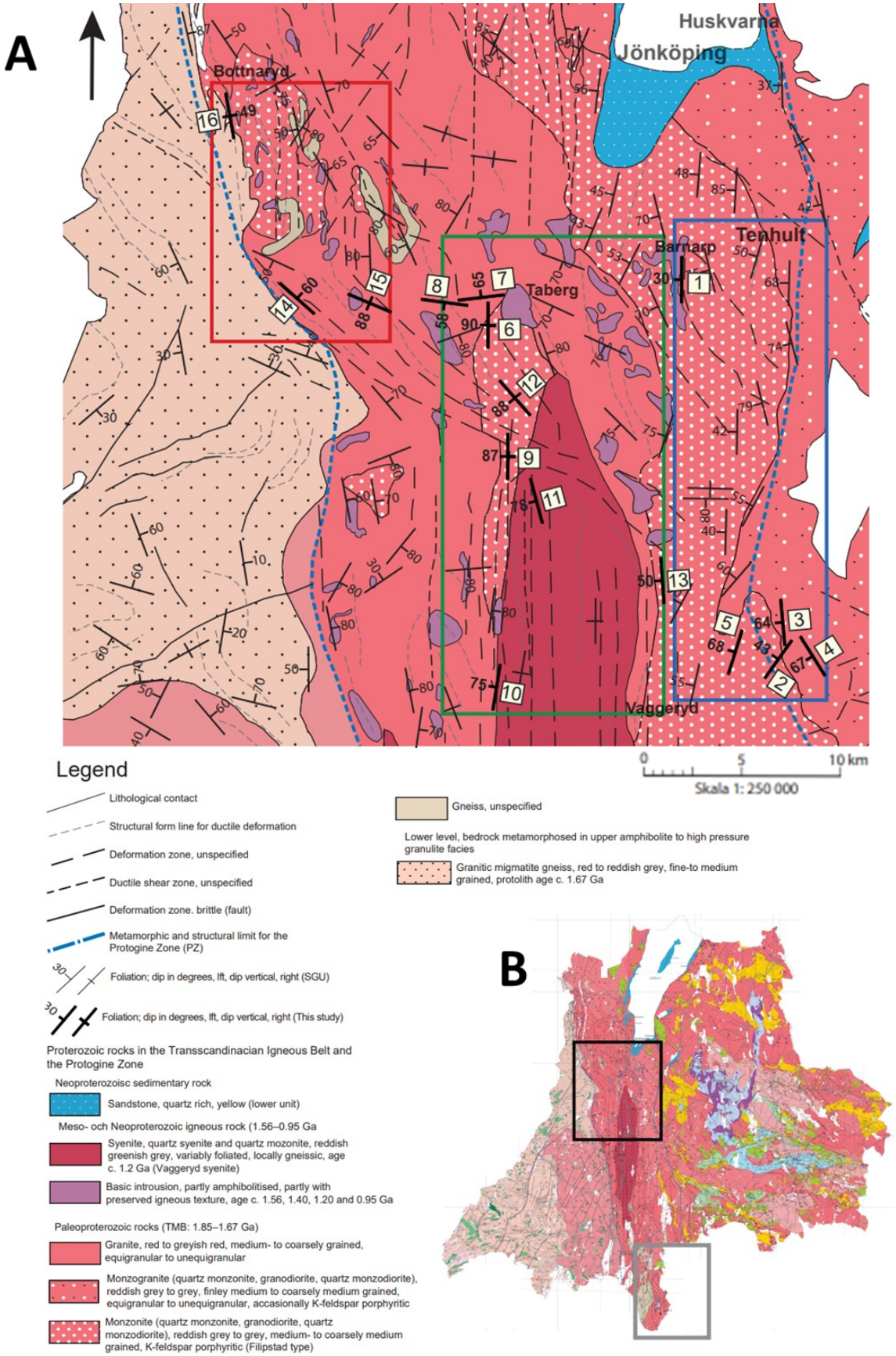

Fig. 4. A) Bedrock geological map, adapted from Wik et al (2006). Blue, green, and red boxes mark the eastern, central, and western subareas investigated in this study, with means of the measured gneissic foliations marked by the bold structural symbols. Thin structural symbols represent data from the SGU. B) Bedrock map of Jönköping county (Wik et al 2006). The black box marks the area of field map A) and the grey box indicates a southern subarea investigated by Perälä (2016).

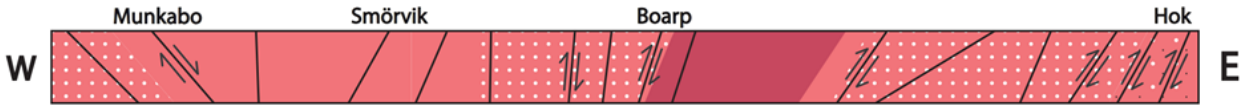

Fig. 5. Schematic W-E profile showing the mean of the measured dip direction from each locality. The western localities are extrapolated southwards to form a W-E profile. The shear sense is mainly interpreted from winged K-feldspar porphyroclasts.

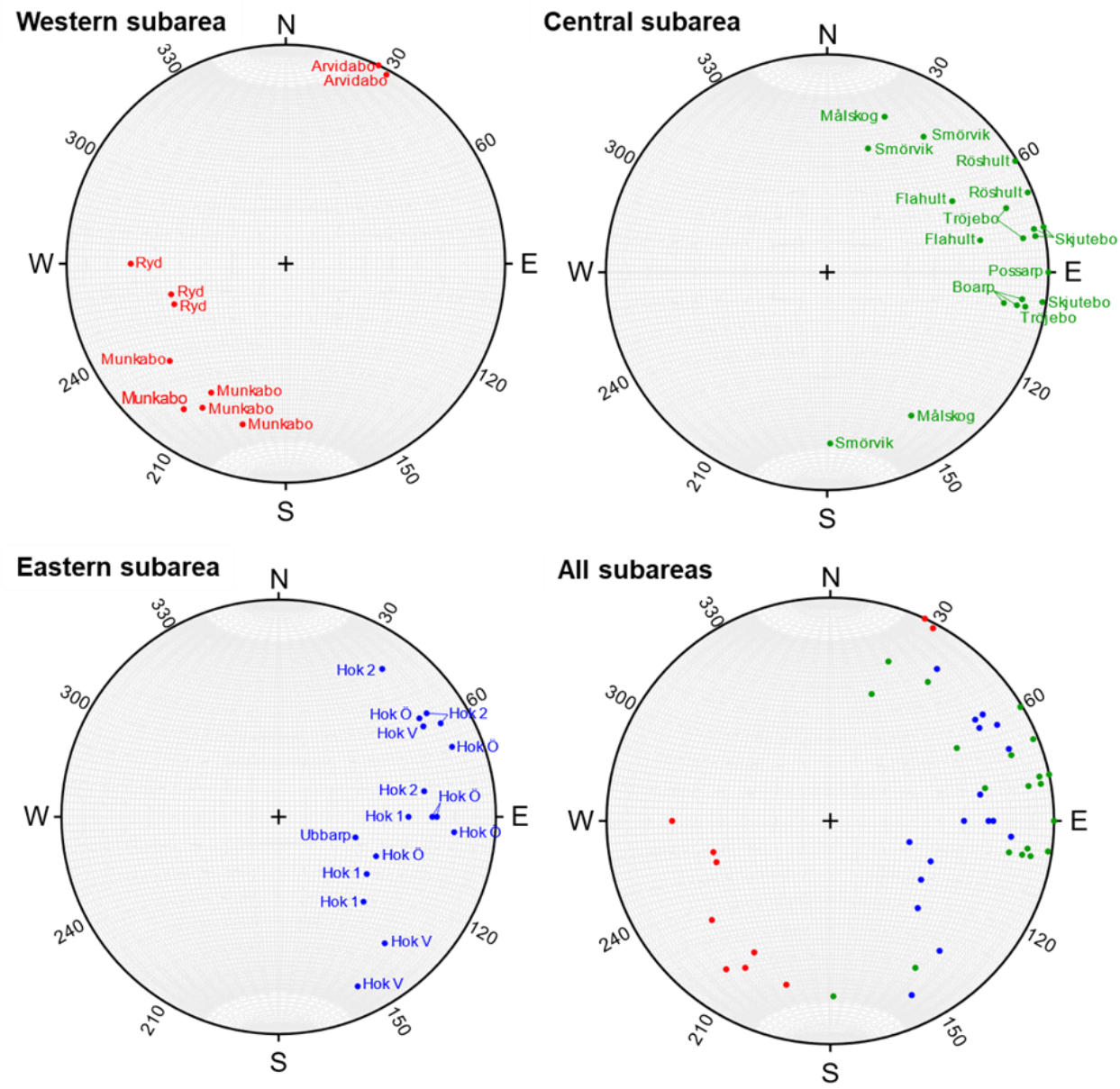

Fig. 6. Schematic W-E profile showing the mean of the measured dip direction from each locality. The western localities are extrapolated southwards to form a W-E profile. The shear sense is mainly interpreted from winged K-feldspar porphyroclasts.

Table. 1. Measured orientations of gneissic foliation (strike and dip) and interpreted sense of shear for the localities investigated in this study. The thin section IDs are included with a note on which are oriented.

Locality	Thin section	X (SWEREF 99 TM)	Y (SWEREF 99 TM)	Orientation	Displacement	References
Ubbarp		6394364	452662	195/30		
	CU19-16A					Uruena et al 2021
	CU19-16B					Uruena et al 2021
Hok 1		6375717	457535	180/ 50	West block up	
				225/ 33		
		6378176	456543	240/ 46		
Mean				215/ 43		
	CU19-05					Uruena et al 2021
Hok Öst		6377279	457132	180/ 62	West block up	
				185/ 70		
				202/ 40		
		6377279	457192	151/ 71		
		6377284	456713	180/ 60		
Mean				175/64		
Hok 2		6375715	457655	145/72	West block up	
	EH21-4.2 (oriented)			125/72		
	EH21-4.22 (oriented)					
		6375827	457596	150/75		
		6375938	457657	170/57		
Mean				147/68		
Hok Väst	EH21-5.0	6375959	455681	148/68		
				245/75		
				230/65		
Mean				208/68		
Possarp		6391921	443445	180/90		
Målskog	EH21-9.0 (oriented)	6392938	442385			
	EH21-9.2 (oriented)			240/65		
		6393375	442988	265/65		
Mean				265/65		
Smörvik		6392724	441786	125/67		
				070/67		
				288/65		
Mean				107/58		
Skjutebo		6386341	444383	168/85		
				170/85		
				168/90		
				182/89		
Mean				172/87		
Boarp	EH21-7.0	6374880	443866	190/76	West block up	
				188/78		
	EH21-7.2 (oriented)			190/70		
Mean				189/75		
Tröjebo		6383093	445773	160/75		
				170/79		
				190/80		
Mean				173/78		
Röshult		6388225	445065	158/87	West block up	
				140/89		
Mean				149/88		
Flahult		6379454	451889	150/45	West block up	
				168/60		
Mean				159/50		
Källarp	CU19-17					Uruena et al 2021
Munkabo		6393399	434101	320/58	West block up	
				305/70		
		6393003	431112	285/65		
				300/57		
				300/65		
Mean				302/60		
Arvidabo		6392780	438028	118/87		
				115/90		
Mean				116/88		
Bottnaryd		6402473	430797	345/45		
				340/45		
		6402475	430737	360/60		
Mean				348/49		
Mjöhult	JP16-03	6296818	460421	N-S (steep)		Perälä 2016
Kalvsjön	JP16-17	6336715	461360	NNW-SSE (78°)		Perälä 2016
Os	JP16-18	6338936	457670	N-S (78° - 90°)		Perälä 2016
Skärsjön	JP16-19	6342812	456287	N-S (78° - 90°)		Perälä 2016
Skaveråsen	JP16-21	6332170	454703	N-S (78° - 90°)		Perälä 2016
Bor	JP16-23	6330040	450999	N-S (78° - 90°)		Perälä 2016

5.1 Field observations

5.1.1 The Eastern subarea

Following are field observations from the 4 localities belonging to the Eastern subarea, marked by the blue box in Figure 4.

5.1.1.1 Ubbarp quarry

The main rock type at Ubbarp quarry (Fig 7a) is a grey-pink granitic gneiss, generally denoted 'Barnarp gneiss'. The rock is coarse- to medium-grained. There is no prominent lineation but a weak to moderate gneissosity defined by the dark mineral aggregates. The gneissic fabric strikes generally N-S and dips about 30 degrees towards the west (Table 1 & Fig 6). The foliation anastomoses around subrounded to elongated K-feldspar porphyroclasts. Recrystallized quartz is furthermore present around these augens. The K-feldspars are relatively intact with few signs of recrystallization and have no or weakly developed tails. The matrix consists mainly of quartz, plagioclase, biotite, and epidote.

5.1.1.2 Hok 1

Light reddish grey 'Barnarp gneiss' is exposed at Hok 1 (Fig 7b). The rock has abundant K-feldspar porphyroclasts and a well-developed foliation striking in N-S and dipping about 43 degrees to the W (Table 1 & Fig 6). The gneissic fabric is anastomosing and defined by elongated K-feldspar porphyroclasts and dark mineral aggregates dominated by biotite and epidote. However, at some outcrops, the fabric is slightly weaker developed. A weak lineation is also generally present in the rock. The K-feldspar porphyroclasts are 0.5–4 cm large and recrystallized quartz form ϕ- and σ-type tailing. Top-to-the-east shear sense has been derived from some porphyroclasts with asymmetric tails at this locality, indicating a movement with the western block up.

5.1.1.3 Hok Öst

At Hok Öst (Fig 7c) pink to grey 'Barnarp gneiss' is exposed as m-scale vaguely folded and relatively steep planes. The moderately distinct foliation strikes N-S, dips about 60 degrees to the W (Table 1 & Fig 6), and is defined by darker minerals. The deformation fabric is at places very prominent with undulating foliation surrounding subrounded to elongated massive K-feldspar augens. In other places, the rock appears slightly more homogenous and massive. K-feldspar porphyroclasts are abundant and prominent everywhere in the rock and are commonly 0.5 – 7 cm large. Recrystallized quartz grains commonly form ϕ- type and σ-type tails of the poprhyroclasts and, the asymmetric tails indicate top – to – south-east and top–to–east shears sense, indicating western block up movement.

5.1.1.4 Hok 2

This is the easternmost locality studied and light pink to pink-grey 'Barnarp gneiss' is the rock type exposed. The relatively thin and prominent foliation is defined by darker minerals such as biotite and epidote. The foliation strikes in NW-SE to N-S and dips about 70 degrees to the W (Table 1 & Fig 6). The lineation in the rock is weak to not distinguishable. The bedrock is furthermore characterized by abundant well elongated K-feldspar porphyroclasts which commonly are mantled by recrystallized blue quartz and plagioclase. The porphyroclasts are relatively homogenous in size, about 0.1 – 0.5 cm large (Fig 7d). Tailed porphyroclasts of ϕ- type and σ- type are common in the rock. The asymmetric tailing indicate top – to – east sense of shear which in turn indicate a movement with the western block up.

5.1.1.5 Hok Väst

At Hok Väst a darker pink to light red 'Barnarp gneiss' is exposed (Fig 7e). The foliation is moderately distinct and defined by darker minerals aggregates of biotite, epidotes, and possibly some hornblende. The strike of the foliation is generally N-S, and the dip is about 70 degrees to the W (Table 1 & Fig 6). The rock is rich in elongated K-feldspar poprhycoclasts which generally are 0.5-2 cm large. Some of the porphyroclasts are mantled by recrystallized quartz which form ϕ- type and σ-type tailing. However, the shear sense of the asymmetric tailing was difficult to distinguish due to weathering of the surface.

5.1.2 The Central subarea

Following are field observations from the 8 localities belonging to the Central subarea, marked by the green box in Figure 4.

5.1.2.1 Possarp

Near-vertical planes of red 'Barnarp gneiss' are exposed (Fig 8a). These are striking in N-S and dipping to the W (Table 1 & Fig 6). The rock is relatively massive, and a prominent deformation fabric is generally not distinguishable. However, at one observation site at the locality, a weak foliation can be seen with the same orientation and dip as the vertical planes, suggesting that the vertical planes represent planes of the foliation. 0,5 – 1 cm large K-feldspar poprhyroclasts is also seen at this observation site and quartz and hornblende are also identified.

5.1.2.2 Målskog

The outcrop in Målskog exposes a weathered surface of red to grey 'Barnarp gneiss' (Fig 8b). The foliation of the bedrock is weak to moderately distinct and defined by dark mineral aggregates of biotite and hornblende with preferred orientation. In places, a weak lineation is also seen in the rock. The strike of the foliation is near W-E, and the dip is 65 degrees to N and W (Table 1 & Fig 6). The surface of the outcrop is relatively steep and has overall the same orientation as the measured foliation, suggesting that the surface is a foliation plane. Aligning with the dark foliation are commonly veins of recrystallized quartz and weak clusters of feldspar porphyroclasts.

5.1.2.3 Smörvik

The exposed rock type at the locality is a pink to grey 'Barnarp gneiss' (Fig 8c). The rock is clearly gneissic and deformed with prominent foliation striking W-E and dipping approximately 60 degrees to the S (Table 1 & Fig 6). Prolonged clusters of darker minerals such as hornblende and elongated vague K-feldspar porphy-

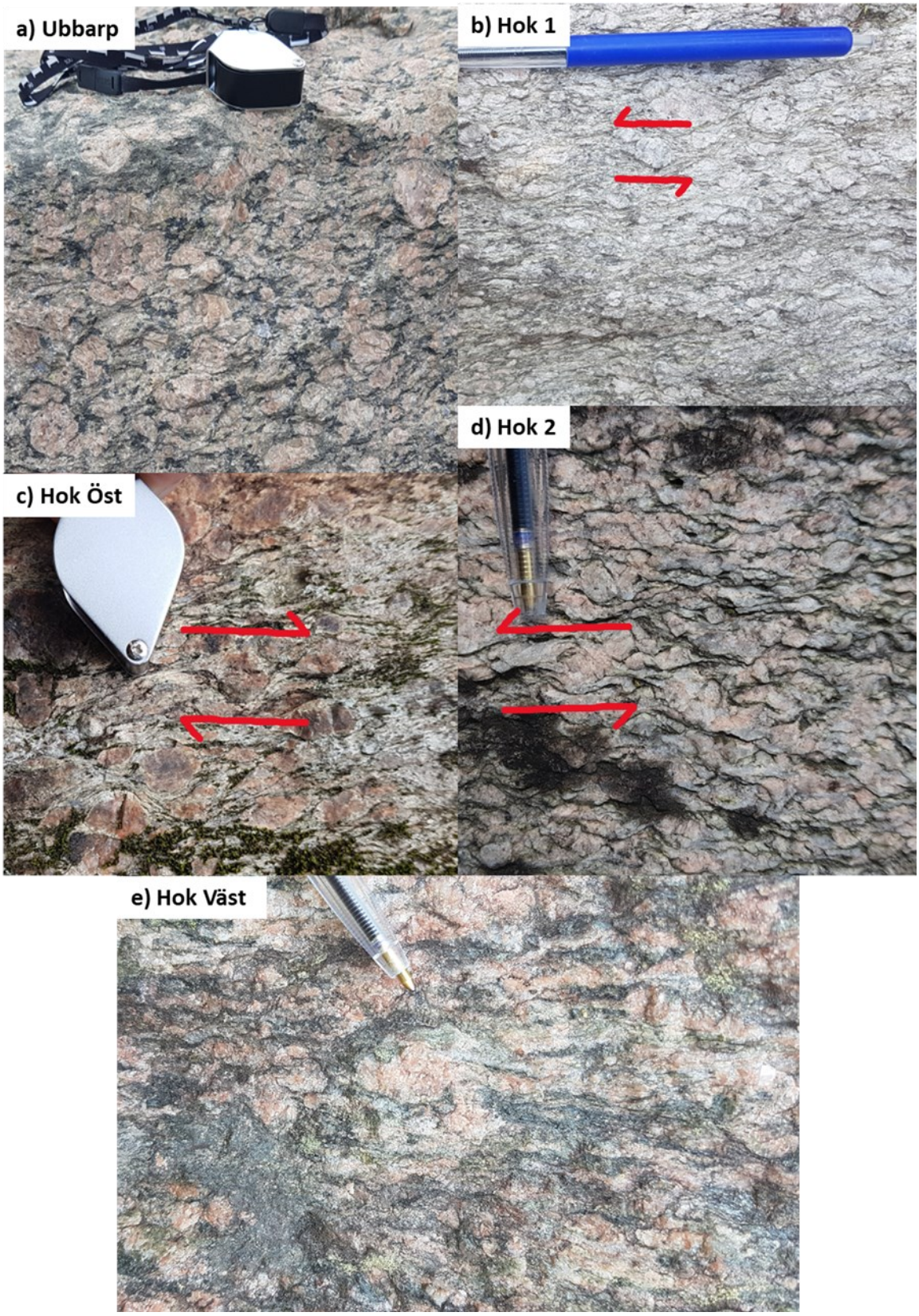

Fig. 7. Field photos of deformed granite "Barnarp gneiss" in the eastern subarea. For scale: hand lens, 4 cm at its length and pen, 14 cm. A) Augen gneiss with coarse K-feldspar porphyroclasts at Ubbarp quarry (locality 1). Near vertical surface. B) Augen gneiss with σ-type porphyroclasts indicating top-to-east shear sense at Hok 1 (locality 2). Near horizontal surface. C) Asymmetric tails on K-feldspar porphyroclasts indicating top-to-southeast shear sense at Hok Öst (locality 3). Steep surface. D) σ-type porphyroclasts indicating top-to-east shear sense at Hok 2 (locality 4). Steep surface. E) Recrystallised K-feldspar porphyroclasts at Hok Väst (locality 5). Steep surface.

roclsts are characteristic of the rock. Commonly are the K-feldspar clasts well elongated and blend into the recrystallized matrix, leaving no prominent augens. At places where the K-feldspar porphyroclasts are distinguishable they have tails of recrystallized quartz and possibly feldspars. Recrystallized plagioclase and quartz are furthermore commonly present in association with the gneissic fabric.

5.1.2.4 Skjutebo

The bedrock exposed is a granitic to syenitic gneiss. The bedrock is light pink and white (Fig 8d), and rich in light-pink feldspar. The near vertical foliation is distinct, defined by darker minerals, and strikes approximate N-S to the W (Table 1 & Fig 6). A lineation is also present in the rock, and it is defined by darker mineral aggregates trending in the orientation of the dip and about perpendicular to the strike of the foliation. The fabric of the rock appears to be deformed, and the minerals are generally very elongated and strained, but no distinct augens are present.

5.1.2.5 Boarp quarry

A light pink to grey-white granitic to syenitic rock is exposed. The quarry walls show consistent steep foliation striking in N-S and dipping to the W (Table 1 & Fig 6). Darker minerals such as biotite, epidote, and possibly hornblende define the foliation and prominent σ-type tailing of K-feldspar porphyroclasts, and at places, ϕ- type are abundant (Fig 9a). Veins of light minerals such as recrystallized quartz and feldspars commonly align with the foliation and mantle porphyroclasts. In some places, a vague S-C fabric and possibly weak C' can be seen. The general shear sense of the asymmetric tailing and the S-C fabric indicates a movement with the western block up. Furthermore, the quarry exposes dm-sized folds, which indicate similar shear sense.

5.1.2.6 Tröjebo

The outcrop exposes a relatively massive, pink to grey granitic to syenitic rock (Fig 9b). In the field, it was not clear if it is the 'Barnarp gneiss' or the 'Vaggery syenite'. The rock has a weak and near vertical foliation defined by clusters of darker minerals. The strike of the foliation is about N-S, and it dips approximately to the W (Table 1 & Fig 6). The lineation of the rock is furthermore also relatively weak. K-feldspar porphyroclasts appear to be less prominent in this locality than in previous. However, recrystallized lighter mineral phases, such as quartz and feldspars, can be detected between the weak distinguishable K-feldspar porphyroclasts. The bedrock is furthermore rich in darker minerals such as biotite and hornblende which commonly make out aggregates with a preferred orientation, similar to the orientation of the cleavages in the bedrock.

5.1.2.7 Röshult

The 'Barnarp gneiss' is exposed and characterized by mylonitic features, distinct and relatively intact K-feldspar augens which are surrounded by a thin foliation within a fine-grained matrix (Fig 9c). The foliation is very prominent and is defined by darker minerals such as biotite. No clear lineation can be seen at this outcrop. The foliation dips near vertically and strikes N-S and NW-SE to the W (Table 1 & Fig 6). The porphyroclasts in the outcrop are subrounded and generally 0.5 – 3 cm large. The frequency of the augens varies within the rock and at places where there are fewer augens the matrix appears more fine-grained. The foliation undulates around the augens and form σ-type tailing which show a top – to -NV shear sense, which indicate a movement with the western block up (Fig 9c). Rims do additionally occur around the porphyroclasts which consist of lighter mineral phases such as recrystallized quartz and plagioclase.

5.1.2.8 Flahult

A light grey 'Barnarp gneiss' is revealed, which at places is well weathered (Fig 9d). The matrix of the rock is generally fine-grained, and the foliation is moderately distinct to weak. The foliation, defined by darker minerals such as biotite and hornblende, strikes near N-S and dips about 50 degrees to the W (Table 1 & Fig 6). K-feldspar porphyroclasts within the rock are elongated and between 0.2-0.5 cm large. The K-feldspar porphyroclasts appear relatively undeformed and no prominent recrystallization of the K-feldspar is visible. However, there are a few porphyroclasts with tails of σ-type and ϕ- type. The asymmetric tailing indicates a shear sense of top-to-SÖ, which suggest a movement with the western block up.

5.1.3 The Western subarea

Following are field observations from the 3 localities belonging to the Western subarea, marked by the red box in Figure 4.

5.1.3.1 Munkabo

A pink to grey 'Barnarp gneiss' is exposed with moderately prominent foliation (Fig 10a). The strike of the foliation is approximate NW-SE and the dip is about 60 degrees approximate to the E (Table 1 & Fig 6). The foliation is defined by darker minerals such as biotite and epidote. K-feldspar augens appear in the rock, and these are between 0.5 to 1 cm large and commonly have tails of recrystallized quartz and plagioclase. Recrystallization of the K-feldspar porphyroclasts also occur in the rock. The tailed porphyroclasts are generally ϕ- type or σ-type and a weak S-C fabric is possibly present in the rock. The shear sense derived from the asymmetric tailing is top-to-east which indicates a movement with the western block up.

5.1.3.2 Arvidabo

The bedrock exposed is a grey to pink 'Barnarp gneiss'. The outcrop shows near vertical foliation planes with weak to moderately distinct foliation fabric on the top surface, perpendicularly to the dipping plane. The near vertical foliation strike about NW-SE to the S (Table 1 & Fig 6) and is defined by darker mineral phases such as hornblende and biotite. The characteristic of this outcrop is a gneissic fabric with well strained K-feldspars, making it difficult to distinguish any distinct K-feldspar augens (Fig 10b). In places, the K-feldspars appear to be recrystallized and recrystallized quartz is frequent in the rock.

Fig. 8. Field of deformed granite "Barnarp gneiss" from the central subarea. For scale: hand lens, 4 cm at its length. A) Near vertical dip of the strong penetrative gneissic foliation in "Barnarp-type gneiss" at Possarp (locality 6). Vertical surface. B) Steeply dipping gneissic foliation in "Barnarp-type gneiss" at Målskog (locality 7). Near vertical surface. C) Penetrative gneissic foliation and recrystallization of "Barnarp-type gneiss" at Smörvik (locality 8). Steep surface. D) Mylonitic gneissic foliation in light pink granitic-syenitic gneiss at Skjutebo (locality 9) Vertical surface.

Fig. 9. Field photos of deformed granite "Barnarp gneiss" from the central subarea. For scale: pen, 14 cm. A) σ-type K-feldspar porphyroclasts indicating western block up shear sense in largely recrystallized Barnarp gneiss at Boarp quarry (locality 10). Near vertical surface. B) Granitic–syenitic gneiss with largely recrystallized feldspars and quartz at Tröjebo (locality 11). Steep surface. C) K-feldspar augen in Barnarp gneiss at Röshult (locality 12). Near horizontal surface. D) K-feldspar porphyroclasts in Barnarp-type gneiss at Flahult (locality 13). Steep surface.

5.1.3.3 Bottnaryd

This is the westernmost locality (Fig 4) and the outcrop here is a mafic rock. The foliation is clearly defined by the lighter minerals aligning in streaks with the preferred orientation. The darker minerals look to be mainly amphibolite and the lighter phases are probably plagioclase (Fig 10c). The strike of the foliation is about N-S, and it dips approximately 50 degrees to the E (Table 1 & Fig 6). Present in the rock in some places is a weak crenulated fabric. The measurable exposures of the mafic rock are limited since some exposures are not accessible, but the overall dip and dip direction looks to be generally the same in the entire area.

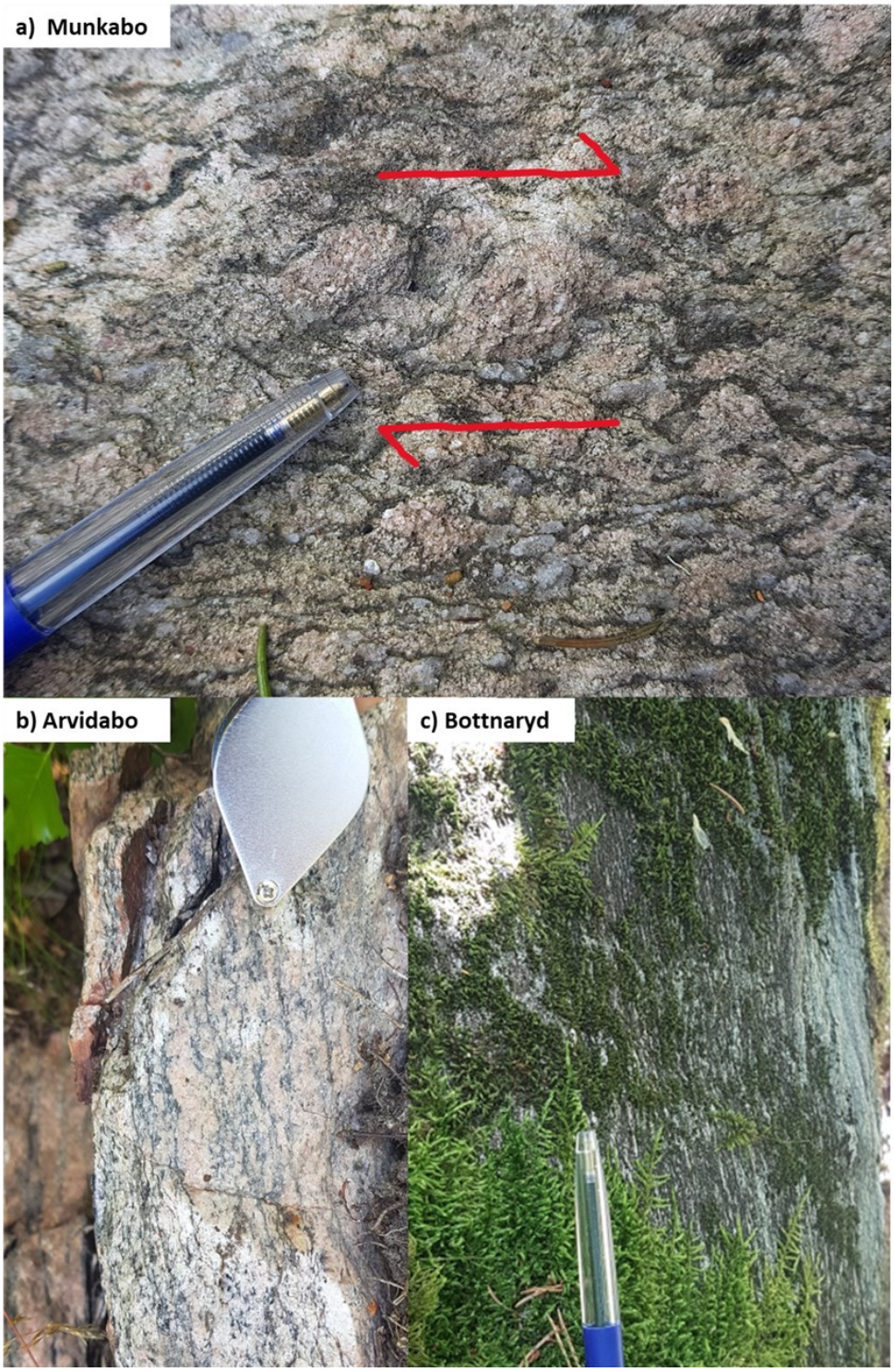

Fig. 10. Field photos of deformed granite "Barnarp gneiss" and metagabbro from the western subarea. For scale: hand lens, 4 cm at its length and pen, 14 cm. A) Recrystallized Barnarp-type gneiss with K-feldspar porphyroclast giving top-to-east shear sense. Munkabo (locality 15). Steep surface. B) Recrystallised Barnarp-type gneiss in Arvidabo with near vertical, penetrative gneissic foliation. Arvidabo (locality 16). Near horizontal surface. C) Strongly deformed metagabbro, with a penetrative gneissic foliation defined by plagioclase (light) and hornblende (dark). Bottnaryd (locality 17). Near horizontal surface.

5.2 Petrography

5.2.1 The Eastern subarea

The samples from the eastern subarea typically have abundant relict feldspars grains with perthitic texture (Fig 11), both seen in samples from Ubbarp (CU19-16A and CU19-16B) (Fig 11a) and in the Hok samples. The relict feldspars are commonly broken and subhedral to anhedral with interlobate grain boundaries. The perthitic texture is often joined by cross-hatched twinning, bent lattice, and undulous extinction in the K-feldspar clasts (Fig 11b). The plagioclase crystals commonly have albite twinning and inclusions of micas and epidote. In all samples recrystallization of feldspar is seen occasionally and indicated by anhedral clasts and neoblast rims around the relict crystals. Recrystallized quartz is more common and indicated by euhedral to subhedral clasts and near granoblastic quartz veins (Fig 11c). The foliation in the samples is prominent, undulating (Fig 11d), and mainly defined by muscovite, titanite, epidote, opaques, and occasionally chlorite and biotite. Sample EH21-5.0 (Fig 11e-f) is rich in large chlorite crystals in contrast to the other samples where the chlorite crystals are relatively rare and small. Urueña et al (2021) have furthermore described sphene, clinozoisite, apatite, and allanite in samples CU19-16A and CU19-16B (Fig 11a) as well as zircon and allanite in sample CU19-05 (11d).

In all samples from the Hok area, porphyroclasts with symmetric tailing can be distinguished and in the EH21-4.2 sample σ-type porphyroclast occur as well. The tails are commonly defined by the foliation and quartz veins (Fig 11g). Mineral fish structures exist in sample EH21-4.22, which indicate top-to-SW which suggest a movement with the western block up (Fig 11h).

5.2.2 The Central subarea

The samples from Målskog (EH21-9.0 and EH-21-9.2) and Boarp (EH21-7.0 and EH21-7.2) do generally appear to have more recrystallized feldspar grains than the samples from the eastern subarea. Igneous feldspars with relict textures (fig 12a) occur but are less common in the central subarea, especially in the samples from Boarp (Fig 12b). Common for all samples in the central subarea are cross-hatched twinning of K-feldspar (Fig 12a), inclusions of micas and epidote in plagioclase, and albite twinning (Fig 12b). In sample CU19-17 from Källarp are undeformed feldspars grain with perthitic texture also common (Fig 12c). Recrystallization of feldspars is however seen in all samples and grain boundary reduction, polygonal grain boundaries, and sub-grain rotation are present. In the Målskog and Boarp samples, the recrystallized fine-grained feldspar commonly appear in aggregates, surrounded by granobalstic quartz. These aggregates are at places also draped by the foliation (Fig 12d-f). The feldspar clasts in the Målskog samples furthermore commonly have a thin rim of neoblasts (Fig 12a) and the feldspars grains in the Boarp samples are near granoblastic at places (Fig 12e & 12g).

All the samples from the central subarea have well-recrystallized quartz with undulous extinction. Granoblastic veins of quartz are prominent and appear undulating, especially in the samples from Boarp (Fig 12g). The quartz veins trend typically E-W, alike the vague foliation defined by mainly biotite, titanite, epidote, and some muscovite. Epidote is notably abundant along the foliation in sample EH21-7.2 and chlorite appears in association with the foliation in the Smörvik samples (Fig 12h). The chlorite is however less abundant than in the samples from Hok in the eastern subarea. Zircon and rutile are also found in the sample EH21-7.2. A few vague porphyroclasts with symmetric tailing appear in sample EH21-7.0 as well as a vague shear band fabric. But no clear shear-sense indicators that can be used to deduce the shear sense are distinguished in the samples from the central subarea.

5.2.3 The Southern subarea

The southern subarea consists of samples from Perälä (2018) and all the samples are from granitic gneissic rocks in the southern Frontal wedge in the study area of Perälä (2018) (Fig 2). The samples are rich in feldspars which at places have perthitic texture (Fig 13a), bent lattices as well as cross-hatched twinning and albite twinning (Fig 13b). Relict and recrystallized feldspars are furthermore seen in most of the samples, but the degree of recrystallization varies between the samples. It seems like the samples from the central-eastern parts of the Frontal wedge such as samples JP16-19 and JP1618 have fewer recrystallized feldspar grains (Fig 13c-e). Anhedral crystal shapes and neoblasts surrounding the feldspars are common in these samples. Samples JP16-21, JP16-23, and JP16-03, which are from the central-western Frontal wedge, are in comparison richer in recrystallized feldspar grains (Fig 13e). In JP16-21 the recrystallized feldspar commonly occur in aggregates mantled by near granoblastic quartz and feldspar neoblasts (Fig 13e). In some places the feldspars appear near granoblastic and in other places bulging and rims of neoblasts are more common (Fig 13f).

Sample JP16-19 has generally a well-developed foliation (Fig 13g) whereas the foliation in the other samples is rather weak and discontinuous. The minerals defining the foliation are mainly micas, epidotes, titanite, as well as chlorite in sample JP16-18 (Fig 13d). The proportion of biotite and muscovite differs however between the samples. Samples JP16-21, JP1623, and JP16-03 are very poor in muscovite (Fig 13f) and JP16-19 is poor in biotite but very rich in muscovite (Fig 13g). Muscovite is also very common in the most eastern sample JP16-17A, which is overall fairly different from the other samples (Fig 13h). The sample is compared to the other samples poor in titanite and biotite as well as recrystallized feldspar grains. Mica fish structures and kinking of muscovite grains are however frequent in sample JP16-17A. According to Perälä (2018), the mica fish structures indicate a movement of the western block up.

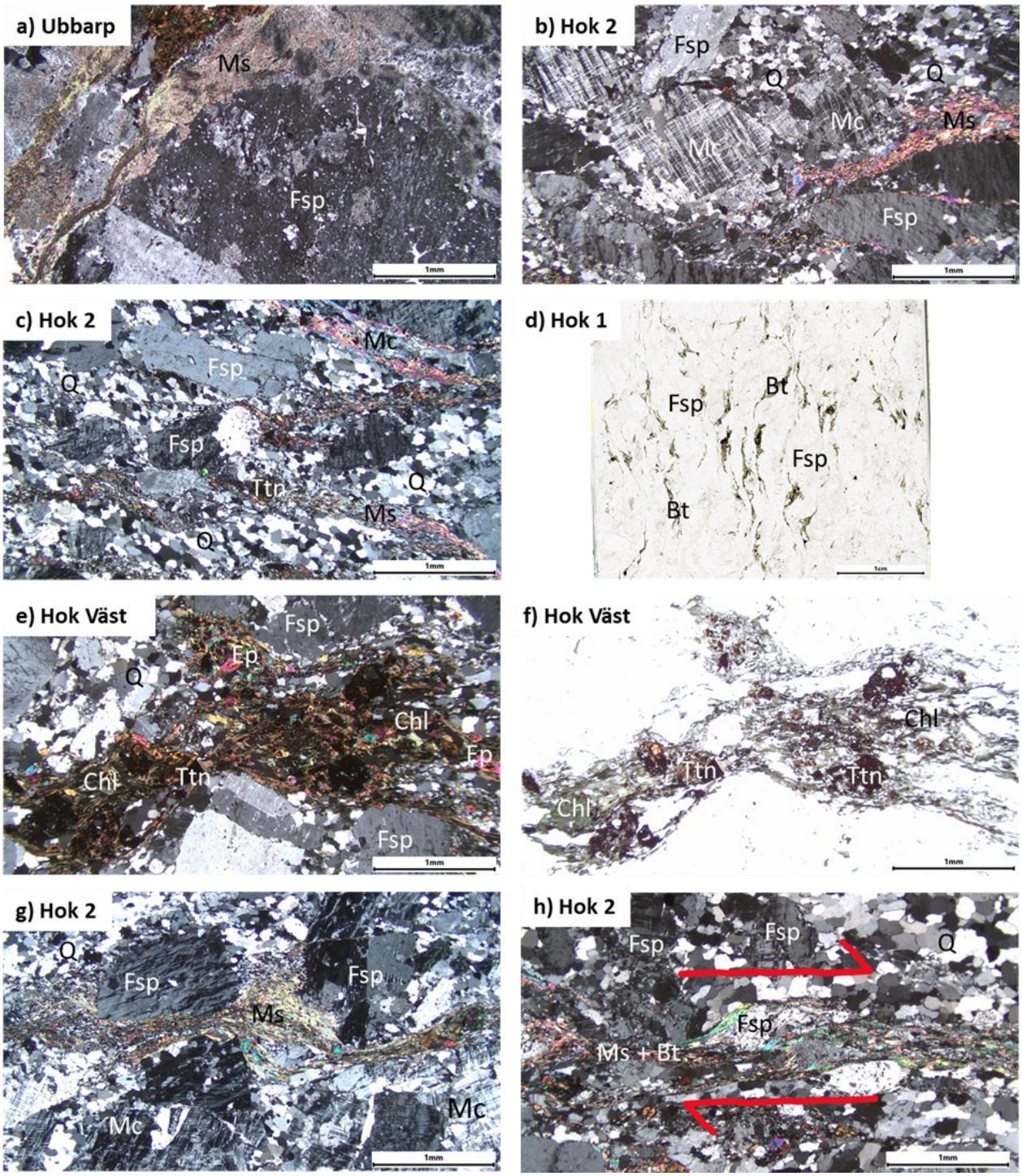

Fig. 11. Photomicrographs of rocks from the eastern subarea, illustrating the minerals and textures related to the deformation. Q: quartz, Fsp: feldspars, Ttn: titanite, Chl: chlorite, Ms: muscovite, Mc: microcline, Bt: biotite, Ep: epidote. A) Igneous feldspar grains with perthitic texture and aggregates of fine-grained metamorphic muscovite and biotite in sample CU19-16A from Urueña et al (2021). B) Relict igneous feldspar grains with cross-hatched twinning and bent lattices in sample EH21-4.22. C) Relict igneous feldspar grains, granoblastic quartz, and foliation of muscovite and titanite in sample EH21-4.2. D) Scanned thin section with anastomosing foliation around larger grains from Urueña et al (2021). Sample CU19-05. E) XPL and F) PPL images of sample EH21-5.0 with foliation of chlorite, epidote minerals, opaques, and titanite in a matrix of relict feldspars and granoblastic quartz. G) Relict igneous feldspar grins, some with cross-hatched twinning. In the center is a σ-type porphyroclast of K-feldspar. Sample EH21-4.2. H) Sigmoidal aggregate indicating western block up movement. Sample EH21-4.22.

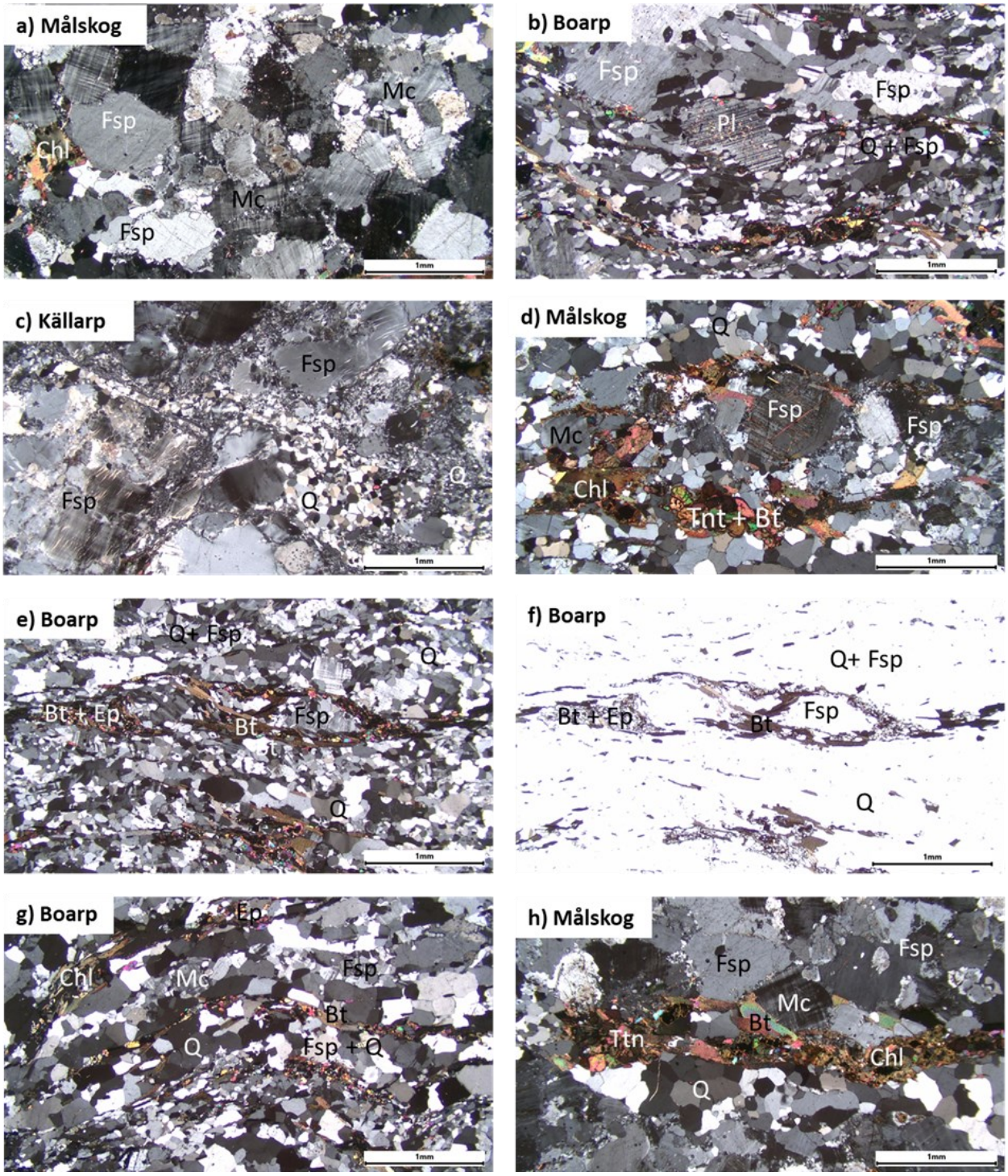

Fig. 12. Photomicrographs of rocks from the central subarea, illustrating the minerals and textures related to the deformation. Q: quartz, Fsp: feldspars, Ttn: titanite, Chl: chlorite, Ms: muscovite, Mc: microcline, Bt: biotite, Ep: epidote. A) Relict and recrystallized feldspar grains, some with cross-hatched twinning and some surrounded by neoblasts. Sample EH21-9.0. B) Feldspar grains with relict textures and perthitic texture. Recrystallized feldspar occur as well. Sample CU19-17 from Urueña et al (2021). C) Plagioclase grain in the center with albite twinning and inclusions of mica and epidote, granoblastic quartz and feldspars surrounding it. Sample EH21-7.0. D) Aggregate of feldspar grains in the center. The larger are igneous and the smaller are recrystallized grains. The foliation is anastomosing around the aggregate and is defined by titanite, biotite, chlorite, and opaques. Sample EH21-9.2. E) XPL and F) PPL images of sample EH21-7.2 with recrystallized feldspar porphyroclast mantled by foliation minerals, mainly biotite and epidote. The matrix is of near granoblastic feldspars and veins of granoblastic quartz. G) Foliation defined by ribbon quartz, biotite, titanite, and epidote. Veins of near granoblastic quartz and feldspars in sample EH21-7.0. H) Foliation of chlorite, biotite, and opaques in a matrix of recrystallized feldspars and elongated domains of granoblastic quartz in sample EH21-9.0.

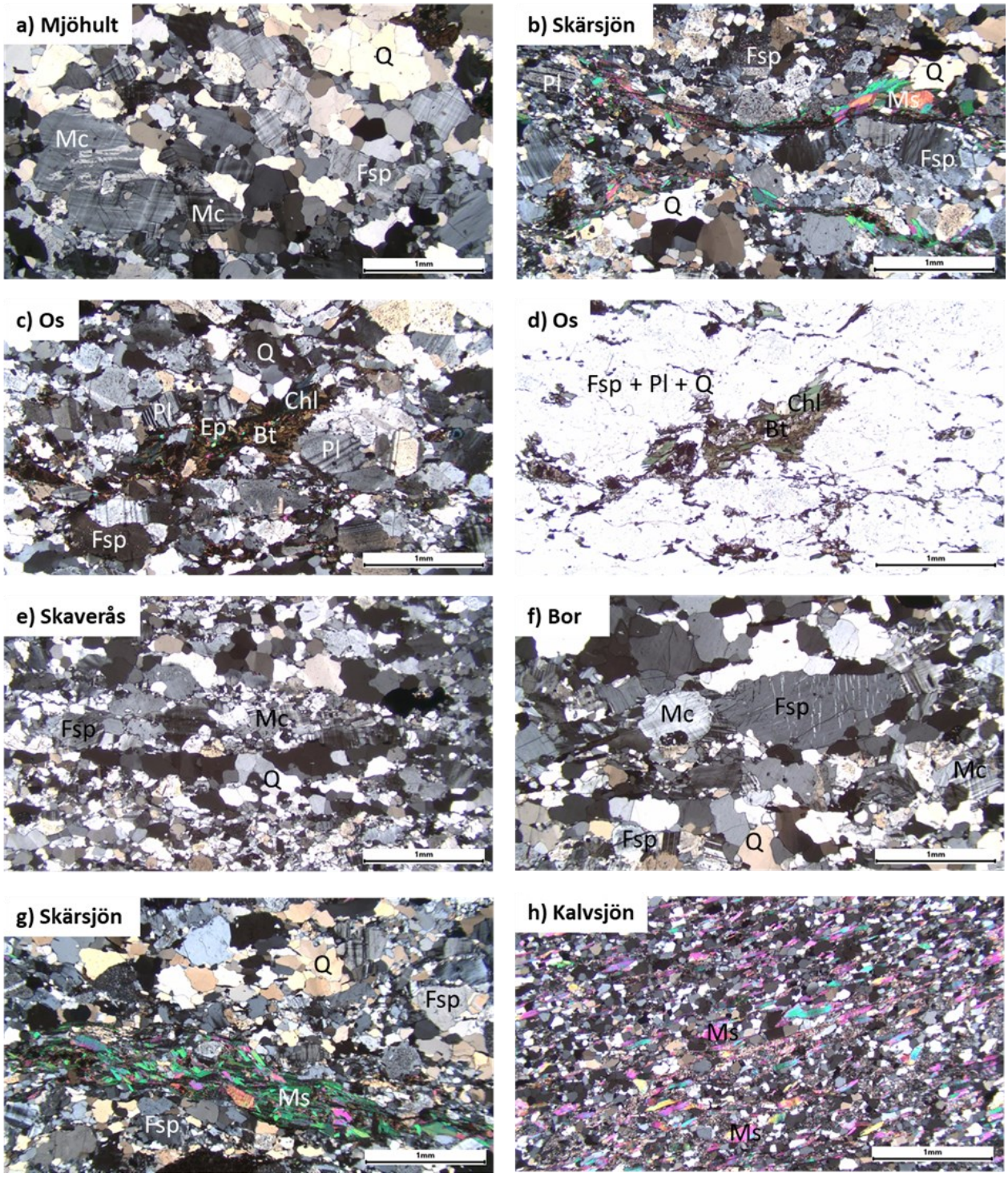

Fig. 13. Photomicrographs of rocks from the southern subarea, illustrating the minerals and textures related to the deformation. Q: quartz, Fsp: feldspars, Ttn: titanite, Chl: chlorite, Ms: muscovite, Mc: microcline, Bt: biotite, Ep: epidote. Samples from Perälä (2016). A) Relict feldspar grains with perthitic texture and cross-hatched twinning. Recrystallized feldspar grains with near granoblastic texture are also present. Sample JP16-03. B) Relict feldspar grains with perthitic texture. Bent lattices of feldspar and plagioclase with albite twinning. Foliation defined by micas and granoblastic quartz. Sample JP16-19. C) Xpl and D) ppl of sample JP16-18. Relict feldspar grains are abundant in this sample but jagged grain boundaries indicate that recrystallized grains occur as well. Aggregate in the center of chlorite, biotite, and epidote. E) Aggregates of recrystallized feldspars. Feldspar grains with cross-hatched twinning, near granoblastic feldspar, and veins of granoblastic quartz, are also present in sample JP16-21. F) Near granoblastic feldspar grains and relict feldspar grains with perthitic texture are present together in sample JP16-23. G) Foliation of micas and matrix of both relict minerals and recrystallized feldspar grains. Sample JP16-19. H) Fine-grained sample rich in micas with sigmoidal shape. Sample JP16-17A.

6 Interpretation and discussion

The results of this study show steep to vertical deformation zones defining a steep belt with a fan- or wedge-like shape across the studied transect. Consistent western-block-up kinematics are found in 7 localities representing all subareas. This indicates normal movement in the western part of the transect and reverse movement in the eastern part. The petrographic studies show that recrystallization of feldspar and penetrative deformation of the rocks increase from east to west, similar to that documented in Möller & Andersson (2018) and Urueña et al (2021).

The model preferred herein recognizes a plausible relationship between the numerous generations of intrusions and the steep structures of the Frontal wedge, similar to what was proposed by Söderlund et al (2005). The pre-Sveconorwegian intrusions, formed at about 1.57 Ga (Ask 1996; Söderlund et al 2005) and 1.2 Ga, (Söderlund et al 2005; Söderlund & Ask 2006) resulted in approximate N-S trending and steep zones of weakness in the crust. These zones of weakness would have paved the way for the formation of the N-S trending deformation zones in the Frontal wedge (Fig 14a). These contacts along the pre-Sveconorwegian intrusions are suggested to have been reactivated during the Sveconorwegian orogeny simultaneous with the development of the main metamorphism throughout the Eastern Segment (Söderlund et al 2005). This interpretation is also in agreement with arguments made by Johansson & Johansson 1990; Johansson (1990), Gorbatschev & Bogdanov (2000), and Söderlund & Ask (2006).

During the Sveconorwegian orogeny, the Eastern Segment was overthrusted by the western Sveconorwegian domain, advancing from the west (Andersson et al., 2002; Möller et al., 2015; Möller & Andersson 2018). The weight on the overtrusted Eastern Segment is proposed to have caused instability within the area of today's Frontal wedge. The response of the rocks within this area, located between rocks impacted by greater vertical pressure in the west and rocks impacted by less vertical pressure in the east, was likely to break along the steep pre-Sveconorwegian zones of weakness (Fig 14b).

The increase of penetrative deformation of the rocks and recrystallization of feldspars from east to west, seen along the studied transect, is suggested to have been caused by the western part of the Frontal wedge being exposed to greater temperatures during the orogeny than the eastern part. This gradational change in the character of the deformation along the studied transect is further proposed to relate to the overall gradational change in deformation and metamorphic grade described in the Eastern Segment by Möller & Andersson (2018).

After about 970–960 Ma, the orogen collapsed and isostatic rebound led to the exhumation of the Eastern Segment (Möller et al., 2015; Möller & Andersson 2018). The exhumation of the Eastern Segment resulted in shear movements along the steep and vertical zones which had been reactivated during the orogeny. It is tentatively inferred that the western part of the area of today's Frontal wedge was buried deeper than the eastern part and that the western block moved up in relation to the eastern. This gave rise to the western-block-up kinematics in the deformation zones, characteristic of the Frontal wedge, and seen in 7 localities (Hok 1, Hok Öst, Hok 2, Boarp, Röshult, Flahult, Munkabo) within the studied area. The Blekinge-Dalarna-Dolorites (BDD), dated at 0.98-0.95 Ga (Söderlund et al 2004), intruded broadly simultaneous with the exhumation of the high-grade rocks in the west, dated at 0.97-0.93 Ga (reviewed in Möller & Andersson, 2018). This argues for that the deformation zones within the Frontal wedge formed in extensional settings, after the main compressional stage of the orogeny (Fig 14c). Further tectonic activity, exhumation, and erosion have exposed the Frontal wedge as we see it today (Fig 14d).

An alternative model proposed for the development of the Frontal wedge was presented by Wahlgren et al (1994). They argue for the occurrence of younger deformation zones, referred to as the Sveconorwegian frontal deformation zone (SFDZ), north and south of lake Vättern. Further, they describe the SFDZ as NNW-SSE and NE-SE striking, younger, ductile, west-dipping deformations zones with reversed and a right-lateral horizontal component of movement. They propose in their model that the SFDZ have caused rotation of the older Sveconorwegian (or older) deformation, resulting in the steep and vertical deformation zones in a fan-shaped structure, that they describe north of lake Vättern. The results presented in this study, show that these steep to vertical fan-shaped deformation zones described by Wahlgren et al (1994) continues even south of lake Vättern. Ductile deformation and, in the eastern to central part of this study area reverse sense of shear, is also described in this study south of lake Vättern. Thus, the studied structures south of lake Vättern do in these aspects resembles the structures described north of lake Vättern by Wahlgren et al (1994). However, the model preferred herein shows a development of the Frontal wedge where a post-Sveconorwegian deformation resulting in the rotation of the older foliation is not needed. I argue thus that this favored model gives a simpler explanation of the formation of the characteristic Frontal wedge features seen south of lake Vättern. The model does also align very well with the research presented regarding the Sveconorwegian orogeny and the development of the Eastern Segment (e.g Möller et al 2015; Möller & Andersson 2018). Furthermore, the model considers the broadly temporal overlap between the intrusions of the BDD and the exhumation of the high-grade rocks in the west. This overlap argues for the Frontal wedge being an extensional structure contrary to what is suggested by Wahlgren et al (1994). The model does further explain the occurrence of the high-grade rocks in the west, described in previous studies within the Frontal wedge (e.g., Möller & Andersson 2018). The rocks in the Frontal wedge were metamorphosed under greenschist-facies in the east and amphibolite-facies in the west (e.g., Möller & Andersson 2018) which indicate a depth of about 35-40 km (Möller et al 2015). Hence, it seems reasonable that the uplift of these rocks influenced the development of the Frontal wedge structures.

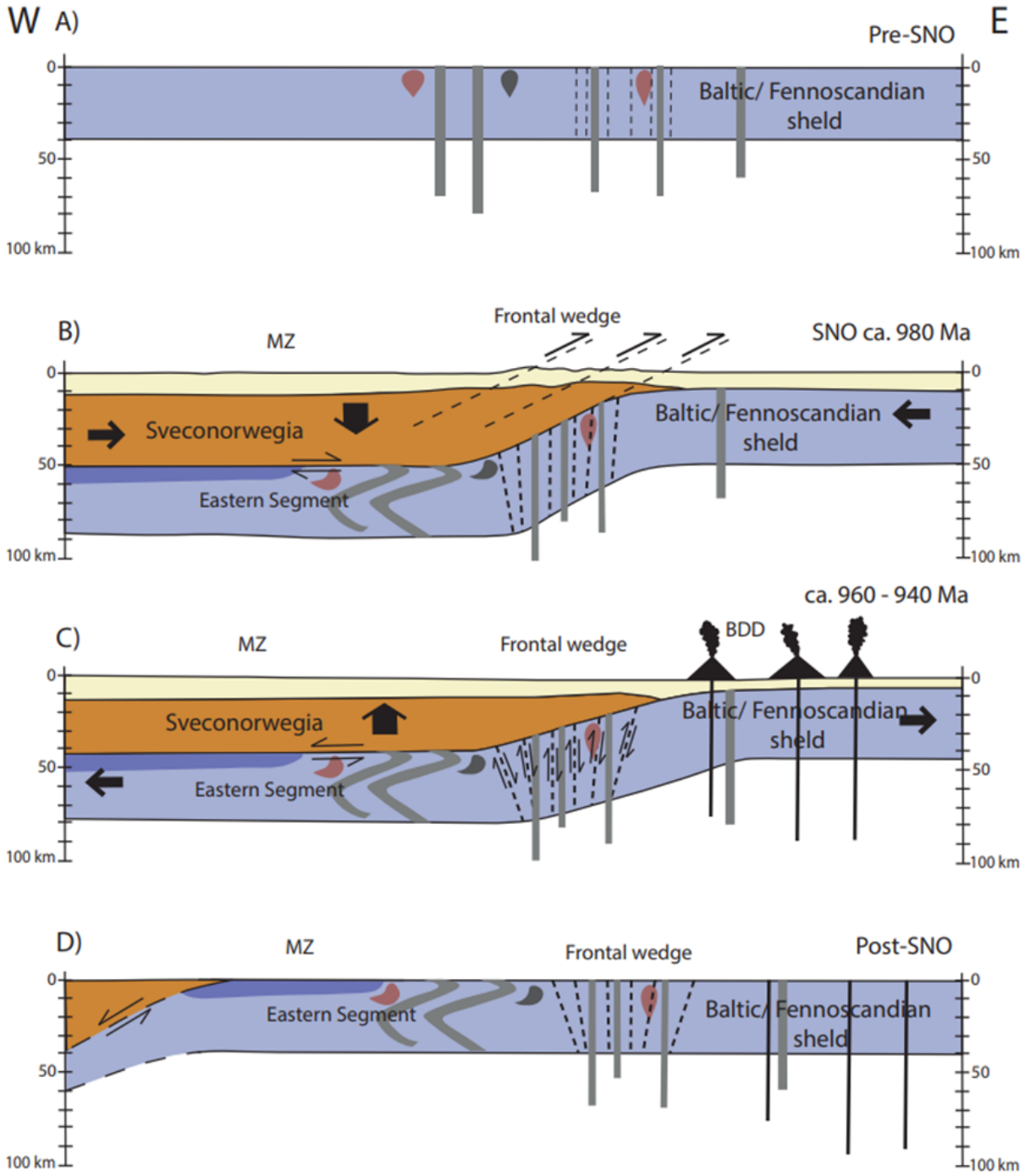

Fig. 14. Proposed tectonic model for the development of the steep deformation structures in the Frontal wedge, following Söderlund et al. (2005) and Möller and Andersson (2018). A) Pre-Sveconorwegian continent Baltica with 1.57 Ga and 1.2 Ga gabbro, syenite, and dolerite intrusions, causing zones of weakness in the crust. B) Himalaya-type crustal thickening with eastwards overthrusting of the western Sveconorwegian domain 'Sveconorwegia'. Regional metamorphism and deformation within the Eastern Segment. C) Extension, intrusion of the Blekinge-Dalarna (BDD) dolerites, and collapse of the orogen at about 960–940 Ma which results in the uplift of the Eastern Segment. This results in western-block-up kinematics along deformation zones in the Frontal wedge. D) Removal of the overburden by extension and erosion has led to the present exposure.

The interpretation argued for here does however not exclude the possibility that younger sets of deformations, like the SFDZ, rrrrr and could have influenced the rocks in the Frontal wedge south of lake Vättern. Rather, I argue that the rotation caused by younger deformations is not necessary to explain the development of the structures that I have observed. With that said, it is possible that the Frontal wedge south of lake Vättern and the structures described further north have undergone different tectonic processes. Local varieties in tectonic movements could possibly have led to the complex belt of deformation seen today. Thus, different models might be applicable for the development of the structure seen in the south and north respectively. Furthermore, there are presumably other aspects and features to the Frontal wedge south of lake Vättern that were not observed during this study, which may impact the interpretation of the tectonic development. Consequently, further studies are still needed to resolve how this complex deformation zone was formed. Dating of the deformation zones would be vital and could possibly test the model of proposed younger deformation zones like the SFDZ suggested by Wahlgren et al (1994). I also suggest that future studies investigate the development of the Frontal wedge structures where an accretionary setting is applied for the Svecorovergian orogeny.

7 Conclusion

- The deformation zones along the transect are steeply dipping or vertical. The dip direction is westwards in the eastern parts of the transect and it changes gradually to vertical and eastwards further west, creating a fan- or wedge-like structure.
- The kinematics of the deformation zones derived from shear sense indicators show an overall western-up-movement throughout the transect: normal movement in the western part and reverse movement in the eastern part of the transect.
- The recrystallization of feldspars and the penetrative deformation increases towards the west, reflecting higher temperatures in the west.
- The studied transect is principally similar to that described from north of Lake Vättern by Wahlgren et al (1994), confirming that a fan-shaped structure continues south of lake Vättern.
- Models aiming to describe the development of the Frontal wedge must consider that steep to vertical deformation zones with western-up kinematics in a fan-like shape are predominant south of Lake Vättern.
- The preferred interpretation of the steep ductile deformation structures south of Lake Vättern is that they accommodated the exhumation of deeply buried western parts of the Eastern Segment during late Sveconorwegian regional extension, after 970–960 Ma. This deformation reactivated previous zones of weakness, including those formed during pre-Sveconorwegian 1. 22 Ga extension and intrusion of dolerites, gabbro, and syenite.

8 Acknowledgments

I wish to thank my supervisors Charlotte Möller and Ulf Söderlund for their guidance and support as well as for all the inspiring discussions throughout the time of this project. This thesis would not have been possible without their input and help. I also wish to thank Cindy Urueña and Jesper Perälä for the opportunity of looking at their samples. I also want to thank the staff at the geolibrary for always cheering for me. A big thanks to all my fellow colleagues at the Department of Geology who gladly have given me feedback and advice whenever I asked for it. Lastly, I want to thank Linnea Halvarsson and Joel Berndtsson for their endless support and encouragement during this time.

9 References

Andréasson, P.-G. & Rodhe, A., 1990: Geology of the Protogine Zone south of Lake Vättern, southern Sweden: a reinterpretation. Geologiska Före ningens i Stockholm Förhandlingar 112, 107-125. Doi: 10.1080/11035899009453168

Ask, R.,1996: Single zircon evaporation Pb-Pb ages from the Vaggeryd syenite and dolerites in the southeastern part of the Sveconorwegian oro gen, Småland, southern Sweden. GFF 118, 8-8. Doi: 10.1080/11035899609546267

Beckman, V., Möller, C., Söderlund, U. & Andersson, J., 2017: Zircon growth during progressive recrystallization of gabbro to garnet amphibo lite, Eastern Segment, Sveconorwegian Orogen. Jorunal of Petrology 58, 167-187. Doi: 10.1093/petrology/egx009

Berglund, J., Connelly, J.N. & Larson, S.Å., 1997: Structural relations, U-Pb geochronology and geochemical character of the Vårgårda Quartz-Monzonite, Eastern Segment of the Southwest Scandinavian Domain, SW Sweden. Ph. D. thesis. Göteborg University, Göteborg, Sweden. 21pp.

Bingen, B., Viola, G., Möller, C., Auwarea, J.V., Lau rent, A. & Yi, K., 2021: Sveconorwegian oro geny. Gondwana Ressearch 90, 273–313. Doi: 10.1016/j.gr.2020.10.014

Bingen, B., Nordgulen, Ø., & Viola, G: 2008a. A four-phase model for the Sveconorwegian orogeny, SW Scandinavia. Norwegian Journal of Geo logy 88, 43–72.

Bingen, B., Davis, D. J., Hamilton, M.A., Engvik, A.K., Stein, H.J., Skår, Ø. & Nordgulen, Ø., 2008b: Geochronology of high-grade meta morphism in the Sveconorwegian belt, S. Nor way: U-Pb, Th-Pb and Re-Os data. Norwegian Journal of Geology 88, 32–42.

Brueckner, H. K., 2009: Subduction of continental crust, the origin of post-orogenic granitoids (and anorthosites?) and the evolution of Fennoscandia. Journal of the Geoogical Society 166, 753-762. Doi: 10.1144/0016-76492008-028

Burke, K., Dewey, J.F. & Kidd, W.S. F., 1977: World distribution of sutures - the sites of former oce ans. Tectonophysics 40, 69-9. Doi: 10.1016/0040-1951(77)90030-0

Falkum, T. & Petersen, J.S., 1980: The Sveconor wegian orogenic belt, a case of late Proterozoic plate collision. Geologische Rundschau 69, 622-647. Doi: 10.1007/BF02104638

Gorbatschev, R. & Bogdanova, S., 2000: Aspects of the Proterozoic boundary between SE and SW Sweden. Department of Geology Lund, Lund, 51 pp.

Hanmer, S., Passchier, C.W., 1991: Shear-sense indi cators: a review. Geological Survey of Canada, Ottowa. 72 pp.

Hansen, B.T. & Lindh, A., 1991: U–Pb zircon age of the Görbjörnarp syenite in Skåne, southern Sweden. Geologiska Föreningens i Stockholm Förhandlingar 113, 335–337. Doi: doi.org/10.1080/11035899109453208.

Henkel, H., 1992: Aeromagnetic and gravity interpre tation of three traverses across the Protogine Zone, southern Sweden. Geologiska Förening en i Stockholm Förhandlingar 114, 344–349. Doi: 10.1080/11035899209454803.

Högdahl, K., Andersson, U. B. & Eklund, O., 2004: The Transscandinavian Igneous Belt (TIB) in Sweden: a review of its character and evolution. Geological Survey of Finland, Special Paper 37, Espoo.

Jarl, L.-G., 2002: U–Pb zircon ages from the Vaggeryd syenite and the adjacent Hagshult granite, sout hern Sweden. GFF 124, 211–216. Doi: 10.1080/11035890201244211.

Johansson, L. and Johansson, A., 1990: Isotope geo chemistry and age relationships of mafic intrus ions along the Protogine Zone, southern Swe den. Precambrian Research 48, 395- 414. Doi: 10.1016/0301-9268(90)90050-Z.

Johansson, L., 1990: The Late Svecononvegian meta morphic discontinuity across the Protogine Zone. Geologiska Föreningen i Stockholm För handlingar 114, 350–353. Doi: 10.1080/11035899209454805.

Juhlin, C; Wahlgren, C.H. & Stephens, M.B., 2000: Seismic imaging in the frontal part of the Sveconorwegian orogen, south-western Swe den. Precmbrian Research 102, 135-154. Doi: 10.1016/S0301-9268(00)00064-4

Laurent, A.T., Duchene, S., Bingen, B., Bosse, V., Seydoux-Guillaume, A.M., 2018b: Two succes sive phases of ultrahigh temperature metamorp hism in Rogaland, S. Norway: evidence from Y-in-monazite thermometry. Journal of Meta morphic Geology 36, 1009–10. Doi: 10.1111/jmg.12425.

Li, Z. X., Bogdanova, S.V., Collins, A.S., Davidson, A., Waele, B. D., Ernst, R.E., Fitzsimons, I.C.W., Fuc, R.A., Gladkochub, D.P., Jacobs, J., Karlson, K.E., Lu, S., Natapov, L.M., Pease, V., Pisarevsky, S.A., Thrane, K. & Vernikov sky, V., 2008: Assembly, configuration, and break-up history of Rodinia: a synthesis. Precambrian Research 160, 179–210. Doi: 10.1016/j.precamres.2007.04.021.

Möller, C., Andersson, J., Dyck, B. & Antal Lundin, I., 2015: Exhumation of an eclogite terrane as a hot migmatitic nappe, Sveconorwegian orogen. Lithos 226, 147-168. Doi: 10.1016/j.lithos.2014.12.013.

Möller, C. & Andersson, J., 2018: Metamorphic zo ning and behaviour of an underthrusting conti nental plate. Journal of Metamorphic Geology 36, 567–589. Doi: 10.1111/jmg.12304.

Passchier, C.W., Simpson, C., 1986. Porphyroclast systems as kinematic indicators. Journal of Structural Geology 8, 831–843. Doi: 10.1016/0191-8141(86)90029-5.

Passchier, C.W., Trouw, R.A.J., 2005. Microtectonics, Second edition. Springer- Verlag, Berlin. 366 pp.

Perälä, J. 2018: Dynamic Recrystallization in the Sveconorwegian Frontal Wedge, Småland, southern Sweden. MSc-thesis Lund University, Lund, Sweden. 36 pp.

Stephen, M.B., Wahlgren, C.H., Weihermas, R. & Cruden, A.R., 1996: Left-lateral transpressive deformation and its tectonic implications, Sveconorwegian orogen, Baltic Shield, sout hwestern Sweden. Precambrian Research 79, 261-279. Doi: 10.1016/0301-9268(95)00097-6

Söderlund, U., Patchett, P.J., Vervoort, J.D. & Isach sen, C.E., 2004: The decay constant of 176Lu determined from Lu-Hf and U-Pb isotope syste matics of terrestrial Precambrian high-temper ture mafic intrusions. Earth Planetary Science Letters 219, 311–324. Doi: 10.1016/S0012-821X(04)00012-3.

Söderlund, U., Isachsen, C. E., Bylund, G., Heaman, L. M., Jonathan Patchett, P., Vervoort, J. D. & Andersson, U. B., 2005: U–Pb baddeleyite ages and Hf, Nd isotope chemistry constraining re peated mafic magmatism in the Fennoscandian Shield from 1.6 to 0.9 Ga. Contributions to Mi neralogy and Petrology 150, 174-194. Doi: 10.1007/s00410-005-0011-1

Söderlund, P., Söderlund, U., Möller, C., Gorbatschev, R. & Rodhe, A., 2005: Petrology and ion microprobe U-Pb chronology applied to a meta basic intrusion in southern Sweden: A study on zircon formation during metamorphism and deformation. Tectonics 23, 1–16. Doi: 10.1029/2003TC001498.

Söderlund, U. & Ask, R., 2006: Mesoproterozoic bi modal magmatism along the Protogine Zone, S Sweden: three magmatic pulses at 1.56, 1.22 and 1.205 Ga, and regional implications. GFF 128,303-310. Doi: 10.1080/11035890601284303

Söderlund, U., Hellström, F. A. & Kamo, S. L., 2008: Geochronology of high-pressure mafic granu lite dykes in SW Sweden: tracking the P–T–t path of metamorphism using Hf isotopes in zircon and baddeleyite. Journal of Metamorphic Geology 26, 539–560. Doi: 10.1111/j.1525-1314.2008.00776.x.

Ulmius, J., Möller, C., Page, L., Johansson, L. & Gan-erød, M., 2018: The eastern boundary of Sveconorwegian reworking in the Baltic Shield, defined by 40 Ar/ 39 Ar geochronology across

the southernmost Sveconorwegian Province. Precambrian Research 307, 201- 217. Doi: 10.1016/j.precamres.2018.01.008.

Uriena, Cindy., Andersson, Jenny., Möller, Charlotte., Lundgren, Linda., Göransson, Mattias., Lin dqvist, Jan-Erik. & Åkeson, Urban., 2021: Va riation in technical properties of granitic rocks with metamorphic conditions. Engineering Geology 293, 2 – 25. Doi: 10.1016/j.enggeo.2021.106283

Wahlgren, C.-H., Cruden, A. R. & Stephens, M. B., 1994: Kinematics of a major fan-like structure in the eastern part of the Sveconorwegian oro gen, Baltic Shield, south-central Sweden. Precambrian Research 70, 67-91. Doi: 10.1016/0301-9268(94)90021-3.

Wahlgren, C.-H., Heaman, L.M., Kamo, S. & Ingvald, E., 1996: U–Pb baddeleyite dating of dolerite dykes in the eastern part of the Sveconorwegian orogen, south-central Sweden. Precambrian Research 79, 227–237. Doi:10.1016/0301-9268(95)00094-1.

Weller, O.M., Mottram, C.M., St-Onge, M.R., Möller, C., Strachan. R., Rivers. T. & Copley. A., 2021: The metamorphic and magmatic record of col lisional orogens. Nature Reviews Earth & Envi ronment 2, 781-799. Doi: 10.1038/ s43017-021-00218-z.

Wik, N. G., Andersson, J., Bergström, U., Claeson, D., Juhojuntti, N., Kero, L., Lundqvist, L., Möller, C., Sukotjo, S. & Wikman, H., 2006: Beskriv ning till regional berggrundskarta över Jönkö pings län. Sveriges geologiska undersökning. Uppsala, 60 pp.

Wikman, H., 2000: Beskrivning till berggrundskar torna 5E Växjö NO och NV. Sveriges Geolo giska Undersökning, Uppsala, 108 pp.

Winter, J, D. 2014: Principles of igneous and Meta moprhic petrology Second edition. Pearson Education Limited, Edinbrugh, 738 pp.

Viola, G., Henderson, I.H.C. ., Bingen, B. & Hendriks, B.W.H., 20011:
The Grenvillian–Sveconorwegian orogeny in Fennoscandia: back thrusting and extensional shearing along the “Mylonite Zone” Precam brian Research 189, 368-388. Doi: 10.1016/j.precamres.2011.06.005

Tidigare skrifter i serien ”Examensarbeten i Geologi vid Lunds universitet”:

589. Olla, Daniel, 2020: Petrografisk beskrivning av Prekambriska ortognejser i den undre delen av Särvskollan, mellersta delen av Skollenheten, Kaledonska orogenen. (15 hp)
590. Friberg, Nils, 2020: Är den sydatlantiska magnetiska anomalin ett återkommande fenomen? (15 hp)
591. Brakebusch, Linus, 2020: Klimat och väder i Nordatlanten-regionen under det senaste årtusendet. (15 hp)
592. Boestam, Max, 2020: Stränder med erosion och ackumulation längs kuststräckan Trelleborg - Abbekås under perioden 2007-2018. (15 hp)
593. Agudelo Motta, Laura Catalina, 2020: Methods for rockfall risk assessment and estimation of runout zones: A case study in Gothenburg, SW Sweden. (45 hp)
594. Johansson, Jonna, 2020: Potentiella nedslagskratrar i Sverige med fokus på Östersjön och östkusten. (15 hp)
595. Haag, Vendela, 2020: Studying magmatic systems through chemical analyses on clinopyroxene - a look into the history of the Teno ankaramites, Tenerife. (45 hp)
596. Kryffin, Isidora, 2020: Kan benceller bevaras över miljontals år? (15 hp)
597. Halvarsson, Ellinor, 2020: Sökande efter nedslagskratrar i Sverige, med fokus på avtryck i berggrunden. (15 hp)
598. Jirdén, Elin, 2020: Kustprocesser i Arktis – med en fallstudie på Prins Karls Forland, Svalbard. (15 hp)
599. Chonewicz, Julia, 2020: The Eemian Baltic Sea hydrography and paleoenvironment based on foraminiferal geochemistry. (45 hp)
600. Paradeisis-Stathis, Savvas, 2020: Holocene lake-level changes in the Siljan Lake District – Towards validation of von Post’s drainage scenario. (45 hp)
601. Johansson, Adam, 2020: Groundwater flow modelling to address hydrogeological response of a contaminated site to remediation measures at Hjortsberga, southern Sweden. (15 hp)
602. Barrett, Aodhan, 2020: Major and trace element geochemical analysis of norites in the Hakefjorden Complex to constrain magma source and magma plumbing systems. (45 hp)
603. Lundqvist, Jennie, 2020: ”Man fyller det med information helt enkelt”: en fenomenografisk studie om studenters upplevelse av geologisk tid. (45 hp)
604. Zachén, Gabriel, 2020: Classification of four mesosiderites and implications for their formation. (45 hp)
605. Viðarsdóttir, Halla Margrét, 2020: Assessing the biodiversity crisis whitin the Triassic-Jurassic boundary interval using redox sensitive trace metals and stable carbon isotope geochemistry. (45 hp)
606. Tan, Brian, 2020: Nordvästra Skånes prekambriska geologiska utveckling. (15 hp)
607. Taxopoulou, Maria Eleni, 2020: Metamorphic micro-textures and mineral assemblages in orthogneisses in NW Skåne – how do they correlate with technical properties? (45 hp)
608. Damber, Maja, 2020: A palaeoecological study of the establishment of beech forest in Söderåsen National Park, southern Sweden. (45 hp)
609. Karastergios, Stylianos, 2020: Characterization of mineral parageneses and metamorphic textures in eclogite- to high-pressure granulite-facies marble at Allmenningen, Roan, western Norway. (45 hp)
610. Lindberg Skutsjö, Love, 2021: Geologiska och hydrogeologiska tolkningar av SkyTEM-data från Vombsänkan, Sjöbo kommun, Skåne. (15 hp)
611. Hertzman, Hanna, 2021: Odensjön - A new varved lake sediment record from southern Sweden. (45 hp)
612. Molin, Emmy, 2021: Rare terrestrial vertebrate remains from the Pliensbachian (Lower Jurassic) Hasle Formation on the Island of Bornholm, Denmark. (45 hp)
613. Höjbert, Karl, 2021: Dendrokronologi - en nyckelmetod för att förstå klimat- och miljöförändringar i Jämtland under holocen. (15 hp)
614. Lundgren Sassner, Lykke, 2021: A Method for Evaluating and Mapping Terrestrial Deposition and Preservation Potential- for Palaeostorm Surge Traces. Remote Mapping of the Coast of Scania, Blekinge and Halland, in Southern Sweden, with a Field Study at Dalköpinge Ängar, Trelleborg. (45 hp)
615. Granbom, Johanna, 2021: En detaljerad undersökning av den mellanordoviciska ”furudalkalkstenen” i Dalarna. (15 hp)
616. Greiff, Johannes, 2021: Oolites from the Arabian platform: Archives for the aftermath of the end-Triassic mass extinction. (45 hp)
617. Ekström, Christian, 2021: Rödfärgade utfällningar i dammanläggningar orsakade av *G. ferruginea* och *L. ochracea* - Problemstatistik och mikrobiella levnadsförutsättningar. (15 hp)
618. Östsjö, Martina, 2021: Geologins

betydelse i samhället och ett första steg mot en geopark på Gotland. (15 hp)

619. Westberg, Märta, 2021: The preservation of cells in biomineralized vertebrate tissues of Mesozoic age – examples from a Cretaceous mosasaur (Reptilia, Mosasauridae). (45 hp)
620. Gleisner, Lovisa, 2021: En detaljerad undersökning av kalkstenslager i den mellanordoviciska gullhögenformationen på Billingen i Västergötland. (15 hp)
621. Bonnevier Wallstedt, Ida, 2021: Origin and early evolution of isopods - exploring morphology, ecology and systematics. (15 hp)
622. Selezeneva, Natalia, 2021: Indications for solar storms during the Last Glacial Maximum in the NGRIP ice core. (45 hp)
623. Bakker, Aron, 2021: Geological characterisation of geophysical lineaments as part of the expanded site descriptive model around the planned repository site for high-level nuclear waste, Forsmark, Sweden. (45 hp)
624. Sundberg, Oskar, 2021: Jordlagerföljden i Höjeådalen utifrån nya borrningar. (15 hp)
625. Sartell, Anna, 2021: The igneous complex of Ekmanfjorden, Svalbard: an integrated field, petrological and geochemical study. (45 hp)
626. Juliusson, Oscar, 2021: Implications of ice-bedrock dynamics at Ullstorp, Scania, southern Sweden. (45 hp)
627. Eng, Simon, 2021: Rödslam i svenska kraftdammar - Problematik och potentiella lösningar. (15 hp)
628. Kervall, Hanna, 2021: Feasibility of Enhanced Geothermal Systems in the Precambrian crystalline basement in SW Scania, Sweden. (45 hp)
629. Smith, Thomas, 2022: Assessing the relationship between hypoxia and life on Earth, and implications for the search for habitable exoplanets. (45 hp)
630. Neumann, Daniel, 2022: En mosasaurie (Reptilia, Mosasauridae) av paleocensk ålder? (15 hp)
631. Svensson, David, 2022: Geofysisk och geologisk tolkning av kritskollors utbredning i Ystadsområdet. (15 hp)
632. Allison, Edward, 2022: Avsättning av Black Carbon i sediment från Odensjön, södra Sverige. (15 hp)
633. Jirdén, Elin, 2022: OSL dating of the Mesolithic site Nilsvikdalen 7, Bjorøy, Norway. (45 hp)
634. Wong, Danny, 2022: GIS-analys av effekten vid stormflod/havsnivåhöjning, Morupstrakten, Halland. (15 hp)
635. Lycke, Björn, 2022: Mikroplast i vattenavsatta sediment. (15 hp)
636. Schönherr, Lara, 2022: Grön fältspat i Varbergskomplexet. (15 hp)
637. Funck, Pontus, 2022: Granens ankomst och etablering i Skandinavien under postglacial tid. (15 hp)
638. Brotzen, Olga M., 2022: Geologiska besöksmål och geoparker som plattform för popularisering av geovetenskap. (15 hp)
639. Lodi, Giulia, 2022: A study of carbon, nitrogen, and biogenic silica concentrations in *Cyperus papyrus*, the sedge dominating the permanent swamp of the Okavango Delta, Botswana, Africa. (45 hp)
640. Nilsson, Sebastian, 2022: PFAS- En sammanfattning av ny forskning, med ett fokus på föroreningskällor, provtagning, analysmetoder och saneringsmetoder. (15 hp)
641. Jägfeldt, Hans, 2022: Molnens påverkan på jordens strålningsbalans och klimatsystem. (15 hp)
642. Sundberg, Melissa, 2022: Paleontologiska egenskaper och syreisotopsutveckling i borrkärnan Limhamn-2018: Kopplingar till klimatförändringar under yngre krita. (15 hp)
643. Bjermo, Tim, 2022: A re-investigation of hummocky moraine formed from ice sheet decay using geomorphological and sedimentological evidence in the Vomb area, southern Sweden. (45 hp)
644. Halvarsson, Ellinor, 2022: Structural investigation of ductile deformations across the Frontal Wedge south of Lake Vättern, southern Sweden. (45 hp)

LUNDS UNIVERSITET

Geologiska institutionen
Lunds universitet
Sölvegatan 12, 223 62 Lund